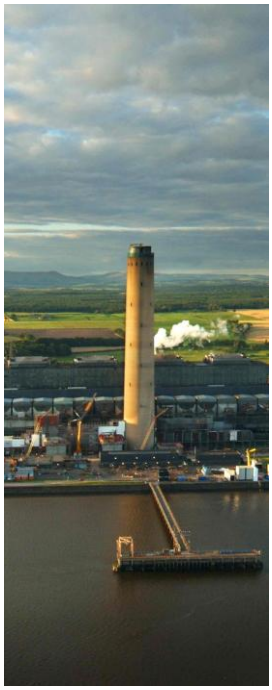

UK Carbon Capture and Storage Demonstration Competition

UKCCS - KT - S7.21 - Shell - 004
CO_2 Storage Estimate

April 2011
ScottishPower CCS Consortium

SCOTTISHPOWER nationalgrid
Carbon Capture & Storage Consortium

UK Carbon Capture and Storage Demonstration Competition

UKCCS - KT - S7.21 - Shell - 004
CO_2 Storage Estimate

April 2011

ScottishPower CCS Consortium

ScottishPower Consortium UKCCS Demonstration Competition

Doc No. UKCCS - KT - S7.21 - Shell – 004 – CO2 Storage Estimate

KEYWORDS

Goldeneye, CO_2, .

Produced by Shell U.K. Limited

ECCN: EAR 99 Deminimus

IMPORTANT NOTICE

Information provided further to UK Government's Carbon Capture and Storage ("CCS") competition to develop a full-scale CCS facility (the "Competition")

The information set out herein (the "**Information**") has been prepared by ScottishPower Generation Limited and its sub-contractors (the "**Consortium**") solely for the Department for Energy and Climate Change in connection with the Competition. The Information does not amount to advice on CCS technology or any CCS engineering, commercial, financial, regulatory, legal or other solutions on which any reliance should be placed. Accordingly, no member of the Consortium makes (and the UK Government does not make) any representation, warranty or undertaking, express or implied as to the accuracy, adequacy or completeness of any of the Information and no reliance may be placed on the Information. In so far as permitted by law, no member of the Consortium or any company in the same group as any member of the Consortium or their respective officers, employees or agents accepts (and the UK Government does not accept) any responsibility or liability of any kind, whether for negligence or any other reason, for any damage or loss arising from any use of or any reliance placed on the Information or any subsequent communication of the Information. Each person to whom the Information is made available must make their own independent assessment of the Information after making such investigation and taking professional technical, engineering, commercial, regulatory, financial, legal or other advice, as they deem necessary.

Table of Contents

Figures

Tables

1. Executive summary

Editor's note:- This report was previously issued at Revision K01. It has been revised to K02 following the outcomes of an Integrated Technical Review held within Shell in March 2011. Revised areas of text and the headings of new figures are highlighted in yellow. The revisions relate to better definition and clarity of presentation of the storage volumes.

Geologic carbon storage capacity has been calculated for the Goldeneye reservoir. The CO_2 storage capacity was initially estimated based on the pore space available for CO_2 injection from a standard volumetric assumption. The method used to estimate the CO_2 storage volume in Goldeneye, a depleted gas reservoir, was hydrocarbon production-based, corrected for CO_2 service. This resulted in a storage volume estimate of **47 million tonnes of CO_2** equivalent available for storage in Goldeneye.

This maximum initial estimate of storage volume was modified by storage efficiency factors, which account for the fact that CO_2 may not be able to completely refill this volume.

An uncertainty analysis study was carried out oriented towards the impact of CO_2 injection, which aimed to deliver a set of parameter ranges and subsurface realisations that need to be modelled (static and dynamic). The outcome of this study suggested that three major static elements could impact the storage capacity of Goldeneye: (a) extension of the stratigraphic pinch-out; (b) structural dip on the western flank of the field; and (c) internal Captain Sand stratigraphy (thickness).

Additional dynamic elements were also considered within the uncertainties that will potentially have an impact on the CO_2 storage capacity of the field. These are mainly related to the displacement mechanism and the unfavourable mobility ratio of the process. These elements were summarized as: (a) relative permeability end points (both water and gas/CO_2), and (b) residual gas saturation (S_{gr}).

The conjunction of these static and dynamic uncertainties depicts the framework which is necessary for understanding the storage efficiency factors that discount the total theoretical capacity.

In addition to the storage capacity defined by the structural trap of Goldeneye, numerical simulation results suggest that the water leg beneath the reservoir (that lies within the storage site) could also account for extra capacity. This is shown in the following figure:-

Storage capacity of Goldeneye for pure CO_2

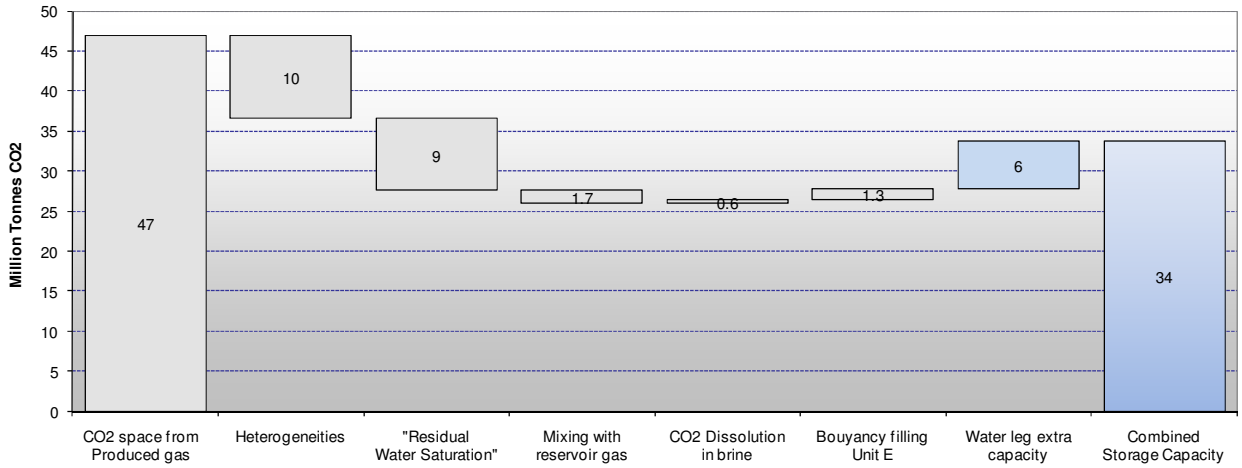

Finally, the discounted analytical storage estimation was compared with the results from a three-dimensional, three-phase, full field Goldeneye numerical simulation model. The objective of this

exercise was to corroborate the initial storage estimations and permit the evaluation of different injection scenarios, in order to map out the range of capacity available for CO_2 storage.

The complete suite of static reservoir models created to investigate CO_2 injection performance in the Goldeneye reservoir was tested. Injection scenarios ranged from:

- A reference case injecting in 4 of the 5 wells available in the field, with an even injection rate for 10 years.
- Extreme cases where all the available CO_2 was injected in a single well
- Injection at double the predicted injection rate

All of these scenarios were investigated in order to demonstrate that Goldeneye has sufficient storage capacity to **hold 20 million tonnes of CO_2,** as mandated by the UK CCS Demonstration Project. All the scenarios showed the field can safely sequester the intended volume with respect to the uncertainties currently evaluated.

In the reference case the injection target was achieved with no backing out of any of the four injection wells and the model indicated just a small proportion (13%) of the total injected CO_2 lying outside the original OWC at the end of injection. However, after cessation of injection all of the CO_2 is either recovered back into the geological store or is otherwise sequestered (via dissolution or capillary trapping).

In order to gauge the maximum geologic carbon storage capacity for the Goldeneye reservoir the simulation models were run with continuous CO_2 injection until 2035 (20 years of injection). These *fill till spill* runs showed that over **30 million tons of CO_2** must be injected to reach the structural spill point and create an egression. The CO_2 was stored both in the Goldeneye hydrocarbon reservoir and also in the aquifer beneath the field. This analysis shows that there is at least a **50% storage capacity margin**, giving confidence that Goldeneye can sequester the 20 million tonnes as mandated by the UK CCS Demonstration Project.

2. Introduction

Depleted oil and gas reservoirs are prime candidates for CO_2 storage for several reasons.

- Oil and gas that originally accumulated in structural and stratigraphic traps was contained (in some cases for many millions of years), demonstrating the long term integrity of such reservoirs.
- The geological structure and physical properties of most oil and gas fields have been extensively studied and characterised.
- Some of the infrastructure and wells already in place may be used for handling CO_2 storage operations.

Goldeneye has all of these elements, making it an excellent candidate for CO_2 storage. However, the ability of the Goldeneye reservoir complex to contain 20 Mt of CO_2 is an important issue.

The Geological carbon storage capacity is an estimate of the maximum amount of carbon dioxide (CO_2) that can be stored in geological formations. The methodologies used to estimate geological carbon storage capacities vary depending upon the specific arrangement of the geologic formation to be used as a storage site. All methodologies start with and estimation of the pore space available for CO_2 injection based on standard volumetric assumptions.

Two main methods could be used to estimate the CO_2 storage volume in depleted oil and gas reservoirs: (1) a volumetric-based CO_2 storage estimate and (2) a production-based CO_2 storage estimate. For the purposes of this assessment, calculation was based on quantifying the volume of hydrocarbons produced (production-based) and assuming that the maximum storage capacity would be given by an equivalent volume of CO_2, where both hydrocarbon and CO_2 volumes were calculated at initial formation pressure. This theoretical maximum volume is modified by storage efficiency factors which account for the fact that CO_2 may not be able to completely fill this volume. In the case of Goldeneye, the need to displace aquifer water that has invaded the reservoir during production is the key consideration.

These storage efficiency factors are specific for each carbon sequestration project and depend mainly on the combination of both static and dynamic features present in the reservoir to be used. During the Goldeneye Project, an Uncertainty Analysis Workshop study was carried out, oriented towards the impact of CO_2 injection, which aimed to deliver a set of parameter ranges and subsurface realisations that need to be modelled (both in the static and dynamic realms). The outcome of this study defined the framework for understanding the storage efficiency factors.

Finally, the analytical storage estimation was compared with the results from a three-dimensional, three-phase, full field Goldeneye numerical simulation model. The objective of this exercise was to evaluate different injection scenarios in order to map out the range of capacity available for CO_2 storage.

3. Objectives and Scope

The objective of this report is to document the geologic carbon storage capacity of Goldeneye, within an uncertainty range based on a collection of parameters, both static and dynamic, that affect the capability of Goldeneye to sequester carbon dioxide.

The ultimate aim is to demonstrate that Goldeneye has sufficient storage capacity to hold 20 million tonnes of CO_2, as mandated by the UK CCS Demonstration Project.

Detailed assessment of the maximum capacity of the depleted Goldeneye field and the adjacent Captain/Koppervik fairway is outside the scope of this report and the UK CCS Demonstration Project.

4. Goldeneye Background & history

In 1996 Shell discovered the Goldeneye field by drilling well 14/29a-3 finding a gas column of 303ft. In the following years three appraisal wells were drilled: 1998 Amerada 20/4b-6 (South), 1999 Shell 14/29a-5 (South-East) and 2000 Amerada 20/4b-7 (South-West). In 2004 five development wells were drilled. The locations of the exploration and development wells are shown in Figure 4-1.

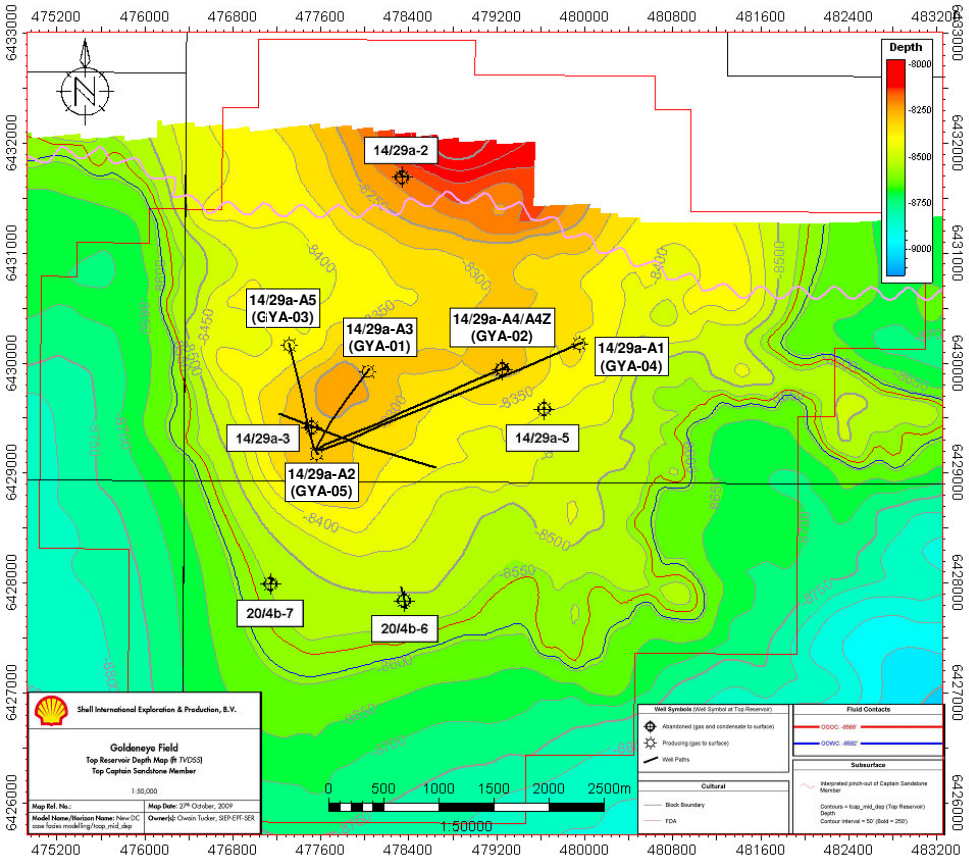

Figure 4-1. Goldeneye well locations.

5. Uncertainty Framework

5.1. Factors influencing the storage capacity of a depleted hydrocarbon reservoir

The major factor influencing storage capacity in depleted hydrocarbon field is the voidage created – i.e. the volume of hydrocarbon and water extracted from the subsurface, less anything injected. Aquifers can flow into fields, however, in so doing they lose pressure – i.e. voidage is created in the aquifer as well.

This initial voidage cannot be completely refilled – there are factors that reduce the volume available and other factors that increase it. The following diagram summarizes the factors impacting the CO_2 storage capacity in a depleted hydrocarbon field – with some specific localisations for the details of the Goldeneye field. A detailed description of this chart can be found in Section 6.

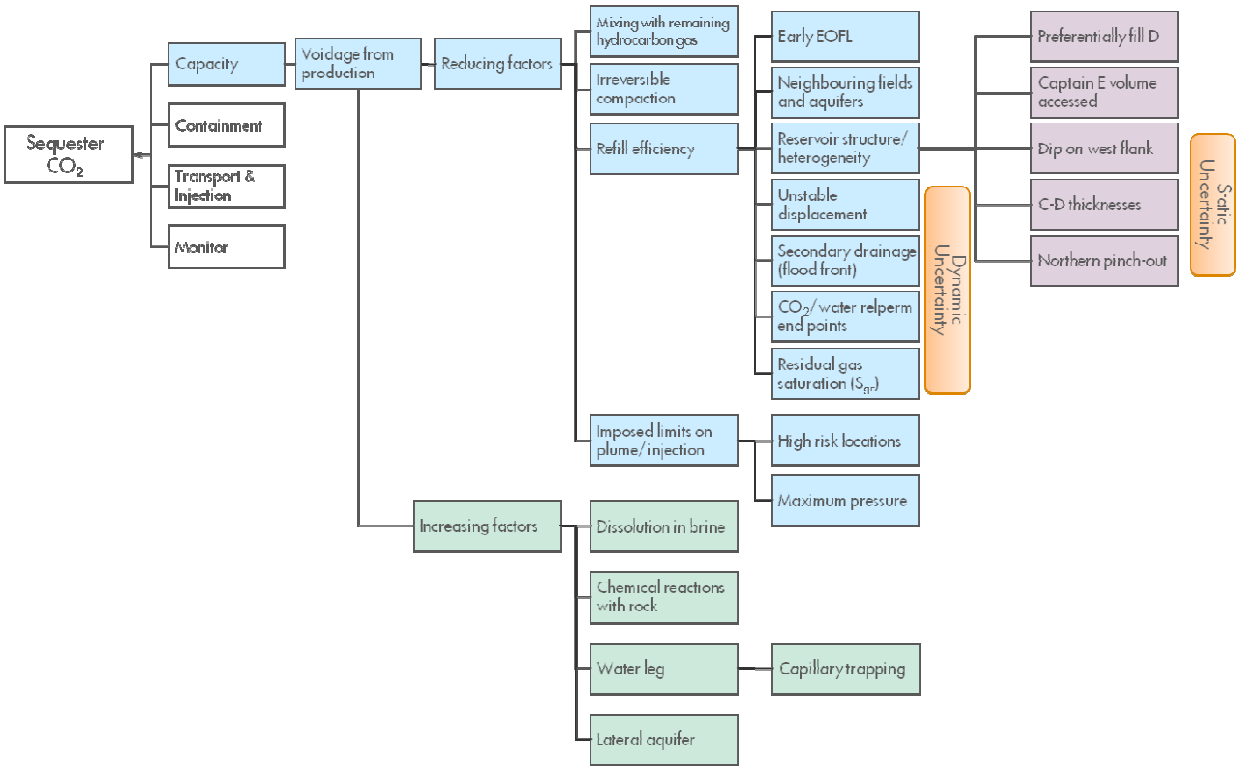

Figure 5-1. Factors impacting CO_2 Storage Capacity.

The general factors outlined in Figure 5-1 need to be assessed against the uncertainties present in the actual hydrocarbon system being reused.

In order to assess the ability of the store to hold 20Mt CO_2 the subsurface uncertainties and the factors impacting CO_2 storage capacity need to be combined to assess the key risks in relation to this volume.

Key uncertainty parameters were classified into two subgroups: *Static* and *Dynamic* (also indicated in Figure 5-1). These will be discussed in the following sections.

5.2. Static Uncertainties in the Goldeneye system

In order to evaluate key uncertainties impacting on CO_2 storage capacity and containment, a suite of static reservoir models was generated which were based upon the data available and the geological understanding of the area. The differences in the models were created by:

- differing seismic depth surfaces to represent the top and base of the reservoir
- using seismic depth surfaces, isochores or well tops to define internal reservoir layering
- varying the location of the northerly stratigraphic pinch-out
- altering the zonation of the pre-reservoir stratigraphy
- adding (or ignoring) a top Captain 'C' pick to well GYA01.

In each case, the data and methodology used to construct the facies and petrophysical property models remained the same – with the exception that the vertical probability curve that controls facies distribution in each zone had to be modified to accommodate changes in zone layering[1]. As a result, several different geological realisations were constructed. The three main aspects identified as key uncertainties with a possible direct impact on CO_2 storage capacity and containment were:

- Extension of the stratigraphic pinch-out
- Structural dip on the western flank of the field
- Internal Captain stratigraphy (thickness)

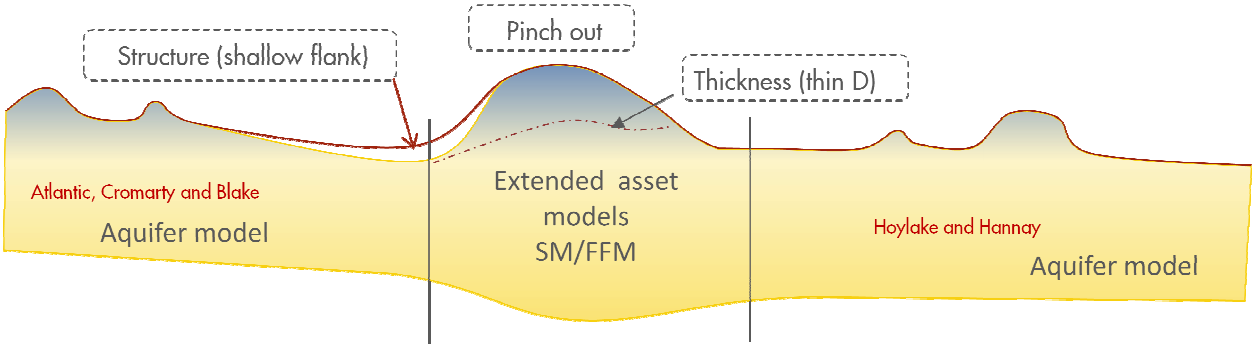

Figure 5-2. Key static uncertainties.

The combination of these three parameters generated the main three geological realisations that were taken into numerical simulation to assess the impact on capacity and containment. Their ranges and relative importance were assessed based on the geological information available.

- Extension of the stratigraphic pinch-out: Precise identification of stratigraphic pinch-out is difficult to achieve, due to scarce well density data from the field. Simulation is therefore required to investigate the impact of the pinch-out location in the CO_2 migration path. In the base case model the position of the pinch-out was selected with the PreSDM seismic data as the basis, with the extreme positions being controlled by the locations of the 14/29a-2 well (which saw no Captain Sandstone Member rocks) and GYA03 and GYA02, (the most northerly of the producing wells, both of which encountered Captain Sandstone Member stratigraphy).
- Structural dip on the western flank of the field: This key uncertainty is based upon uncertainty in the velocity model. Alternate supra-Beauly wedge interpretation sees the 'supra-Beauly

[1] Static reservoir modelling (field) report for CO_2 in Goldeneye project. Doc No. FM020D3 (RT 060)

wedge' migrated 750m to the west. This has the effect of reducing the structural dip on the western side of the field.

- Internal Captain stratigraphy (thickness): two scenarios of internal Captain stratigraphy were considered. One scenario is generated when using constant isochors to create the reservoir zones, whilst the second scenario is associated with the use of well tops without isochores or seismically interpreted surfaces to divide the reservoir. This sensitivity has a large impact on the size of the in-place hydrocarbon volumes in the internal zonation of the reservoir. Reallocating volume between the high net-to-gross 'D' unit and the low net-to-gross 'C' unit can change the in-place volume between -9.6% and +4.8%[2]. As well as changing the size of the reservoir from which gas is being produced, this reallocation of rock volume will affect the full field simulation, swapping volumes between an easily accessible, high quality container and a less easily accessed, low quality one.

However, it is important to mention that geologic realisations with seismically interpreted surfaces were tested and it was not possible to achieve a history match. As a result, the models carried over were executed using constant isochors to create the reservoir zones.

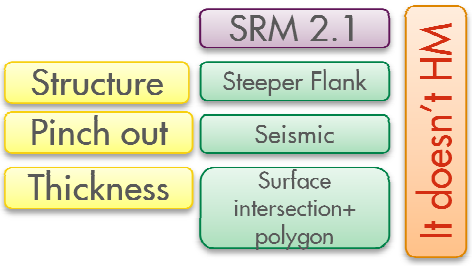

The following static uncertainty matrix summarises the scope of the study regarding this topic.

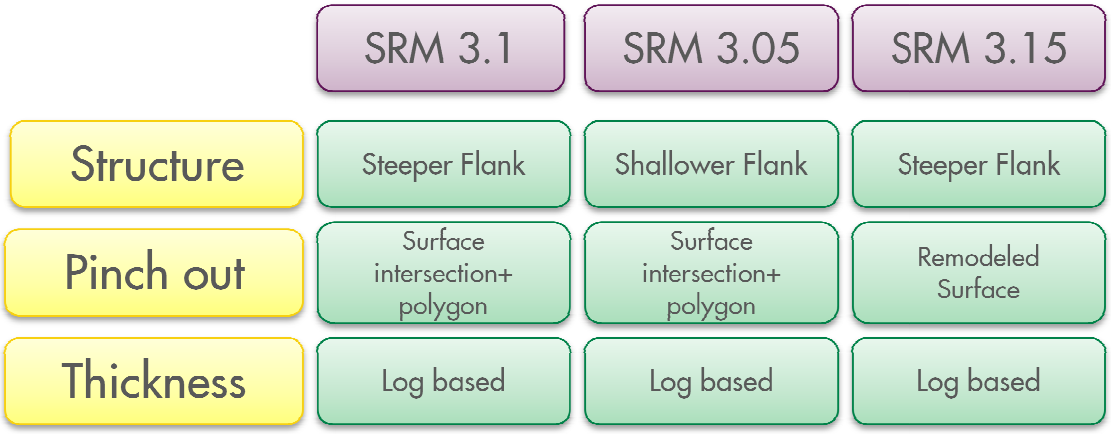

Figure 5-3. Static uncertainty matrix.

Study of these key uncertainty elements is expected to result in assessment of the following:

- Structural dip on the western flank of the field: impact of the structure in the displacement process. Degree of instability of the CO_2 – water displacement process (Dietz tongue effect) with respect to the steepness of the west flank of the field, Taking into account the fact that a shallower flank will produce less gravity force to overcome when CO_2 is trying to reach the lowest structural point and escape out of the reservoir.
- Extension of the stratigraphic pinch-out: the precise geometry of the pinch-out and north boundary of the field, which is not accurately known, could have an impact in the possible

[2] Initially In-Place (IIP) Volumes report for Goldeneye project. Doc No. SP-FM020D3

lateral egression of CO_2. The geometry has an impact in the hydrocarbon volumes at the north-west corner of the field (the effects can produce a maximum reduction in GIIP of -5.3% and a maximum increase in volumes of +1.2%) and as a consequence, the CO_2 storage capacity and migration path.

- Internal Captain stratigraphy (thickness): this will also have an impact on hydrocarbon in place (change the in-place volume between -9.6% and +4.8%) and its distribution among the reservoir units, probably again impacting CO_2 storage capacity and the migration path or accumulation.

The understanding of all of these static uncertainties in conjunction with dynamic variables, will inform project decisions such as the injection strategy, the injection well priorities, well completion designs, measurement, monitoring and verification strategies, and others.

5.3. Dynamic Uncertainties in the Goldeneye system

In addition to this set of static uncertainties, a series of dynamic parameters were also considered. The main concern from the fluid dynamics of CO_2 injection was related to the displacement processes that will occur within the reservoir.

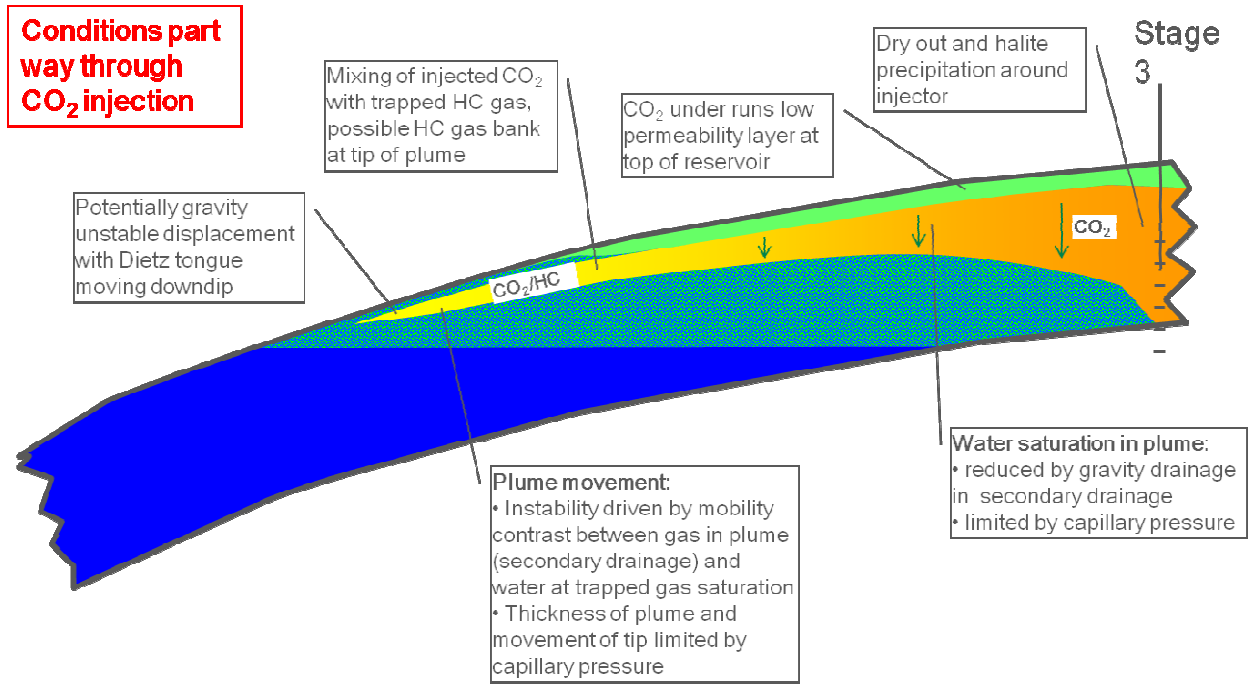

Figure 5-4. Displacement process in Goldeneye lifecycle.

At Goldeneye pressure and temperature, the CO_2 dense phase is less dense than water and so under equilibrium conditions it will overlay the brine filled part of the reservoir. However during injection, the CO_2 displaces water under segregated flow conditions and can tongue and override the water (Dietz instability).

This will lead to a set of dynamic uncertainties dominated by relative permeability parameters such as:

- Relative permeability end points (both water and gas/CO_2)
- Residual gas saturation (S_{gr})

There could be additional dynamic uncertainties having an impact in the displacement such as:

- Oilrim
- kv/kh ratio

However, these will be constrained by the history match of the model.

In the displacement of water by CO_2 injection at the top of the structure and interval, the interface between the fluids will be strongly gravity dominated simply due to density difference.

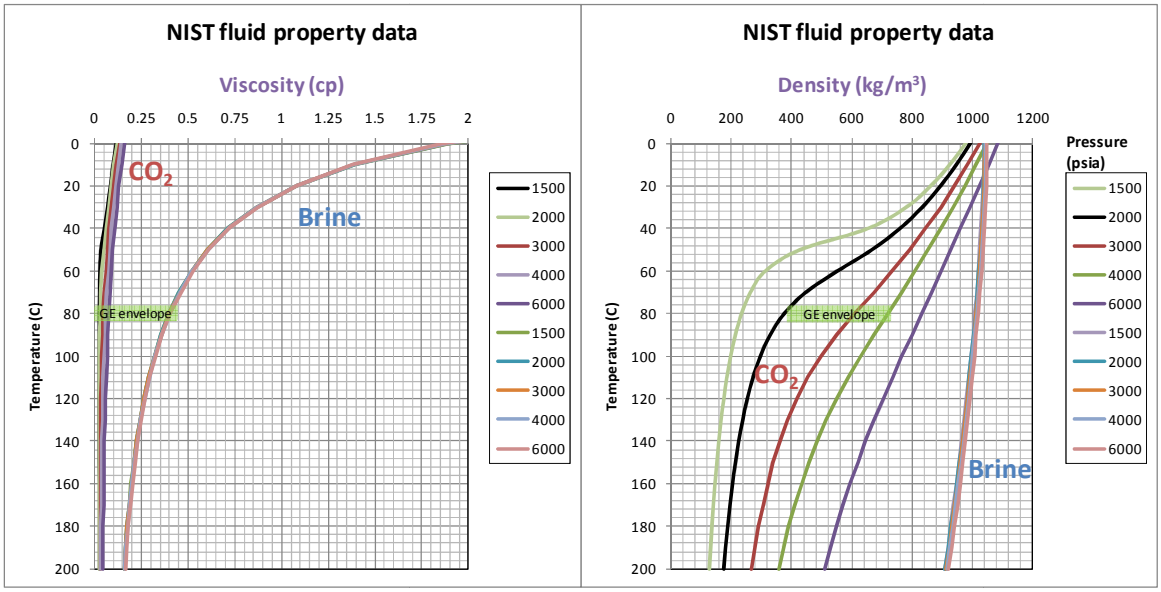

Figure 5-5. CO_2 and Water viscosity and density vs. pressure and temperature.

As may be seen, pure water viscosity is strongly dependent upon temperature, but this is not the case for CO_2. Study of the density plot shows that CO_2 density is strongly dependent on pressure/ temperature, but this is not the case for water. These general physical behaviours of both water and CO_2 will have a predominant impact on the way in which the CO_2 plume will behave, allowing worse or better displacement due to the viscosity ratio of the fluids.

The density of supercritical CO_2 is around 40 – 50 % lower than typical saline formation water under the same conditions. As a result of this density difference the lighter CO_2 will want to rise upwards, driven by buoyancy through the formation to accumulate at the highest possible place in the reservoir beneath the seal.

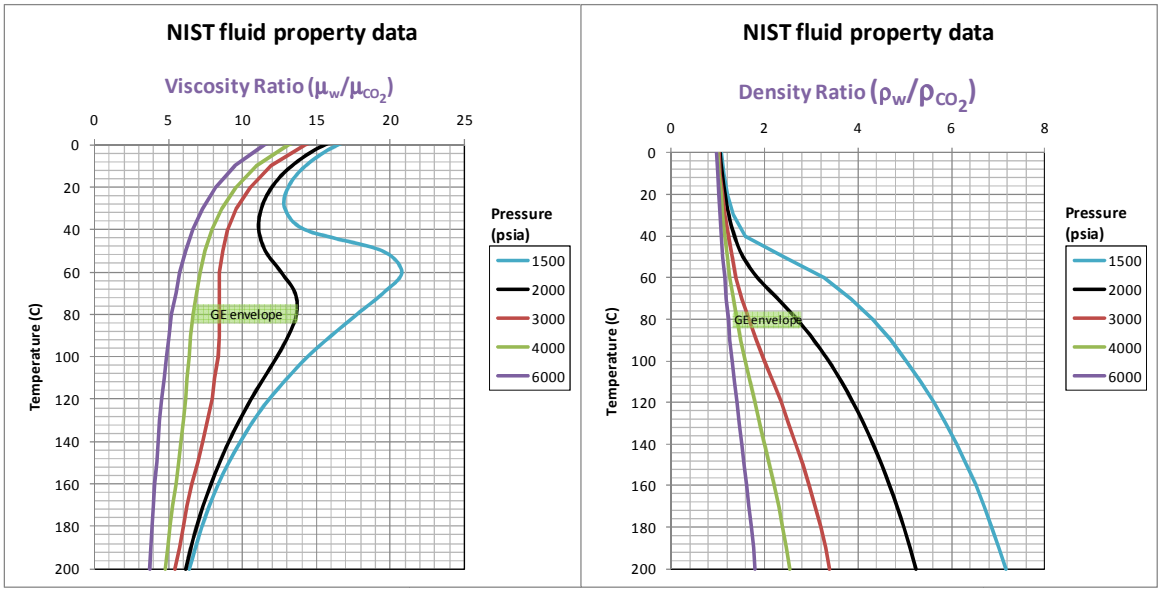

Figure 5-6. Viscosity and Density ratio as a function of pressure and temp.

This mobility ratio contrast between gas in the plume (secondary drainage) and water at trapped gas saturation will enhance the instability of the displacement. Estimations at reservoir conditions revealed that a highly unfavourable mobility ratio in the order of 25 will be achieved.

During displacement under segregated flow conditions, in the manner foreseen in Goldeneye, it is expected that in the flooded part of the reservoir CO_2 alone will be flowing in the presence of residual water saturation. In this condition the effective permeability $k_{rg} = kk_{rg}'$, where k_{rg}' is the end point relative permeability to water (water will carry on draining under gravity). In the unflooded zone, water will be flowing in the presence of residual gas saturation with effective permeability $k_{rw} = kk_{rw}'$, where k_{rw}' is the end point relative permeability at S_{gr}.

Different sets of relative permeability curves were implemented in order to assess the impact on the displacement.

Special Core Analysis (SCAL) data currently available in the field is as follows[3]:

- Well 14/29A-3 and 14/29A-5
  - Corelabs study for Shell
  - Steady state imbibition gas/water relative permeability
- Well 20/4b-6
  - Corelabs study for Amerada Hess
  - Wettability (well encountered oil rim)
  - Steady state imbibition gas/oil, SS drainage gas/oil, SS imbibition water/oil
- Well 20/4b-7
  - Study for Amerada Hess
  - Report on SCAL programme requested

Land correlation for Captain D, using "corrected data" gives a range of residual gas saturation (S_{gr}) of 25% - 38% at maximum gas saturation.

[3] SCAL Report for Goldeneye project.

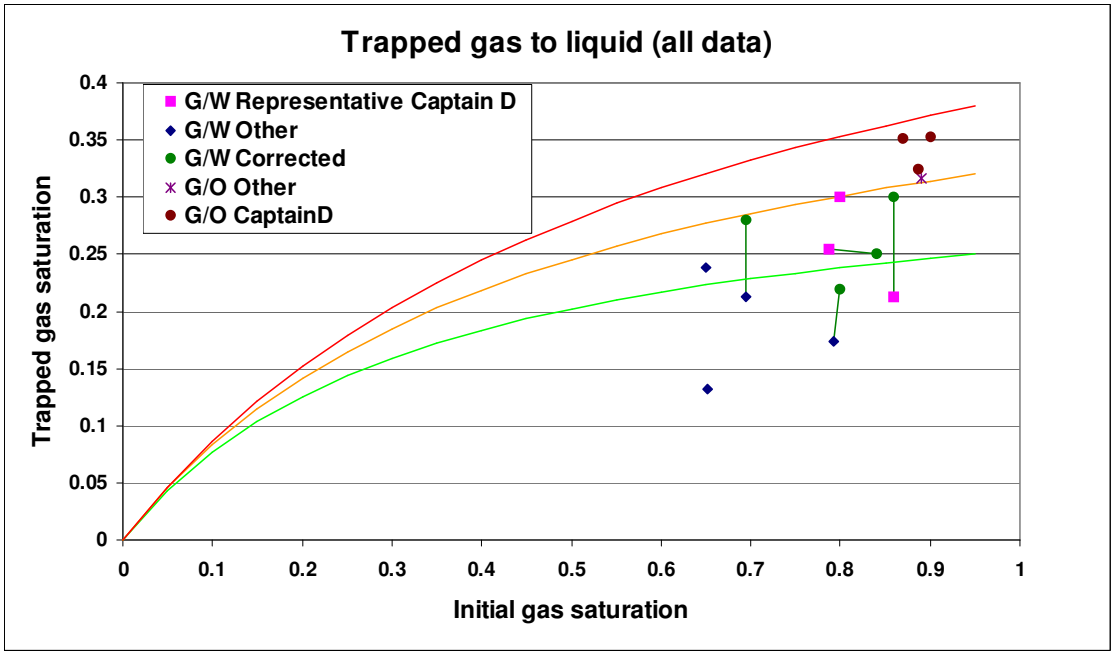

Figure 5-7. Trapped gas saturation to liquid. Land correlation.

Also, data taken from literature shows a strong correlation between porosity and residual gas saturation. So for an average porosity of ~24% measured in Goldeneye Captain D, the residual gas saturation can be ~30%. For the sensitivity analysis carried out in the simple box model, hysteresis in gas relative permeability was set up with S_{gr}=30%.

Additionally, there is uncertainty in the water relative permeability end point. Various sensitivities were performed to investigate this, with gas relative permeability and all other parameters held constant. Water relative permeability end point values, based on data currently available in the field that do not require correction, support a range of 0.05 to 0.25. Corrected data means that instead of using the average water saturation measured along the core, which in some cases was very variable and not representative of in situ conditions, closest value to S_{wi} was chosen and the correspondent S_{gr} value was assumed to be correct.

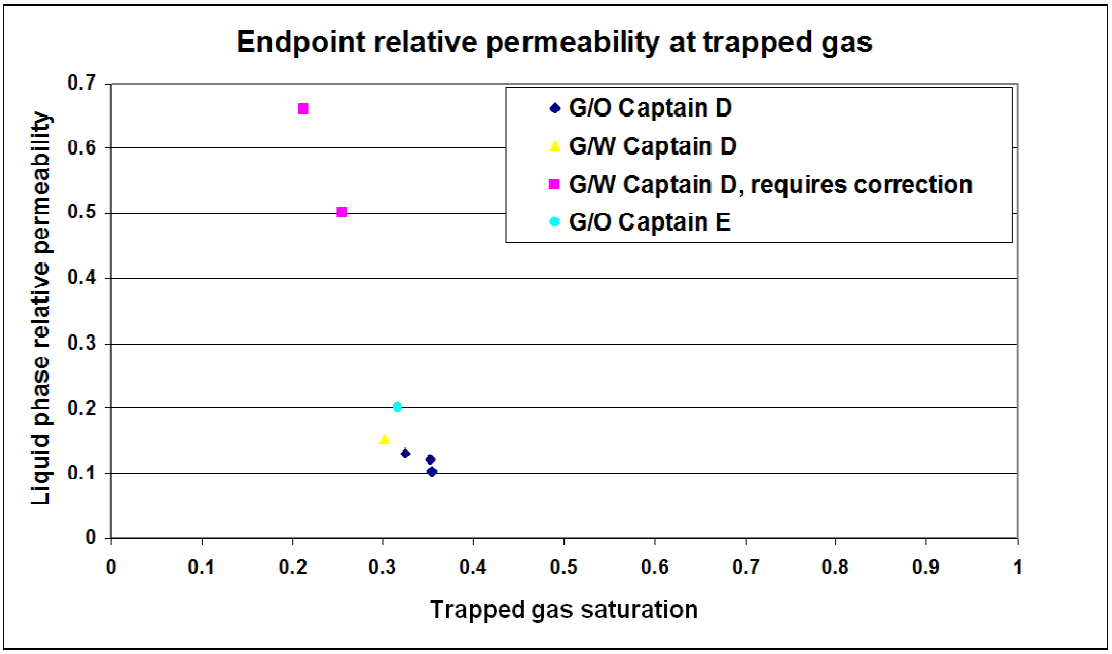

Figure 5-8. Endpoint relative permeability at trapped gas saturation.

Dynamic uncertainty parameters were investigated mainly in a simple box model and not the FFM. This allowed a better understanding of their impact in a mechanistic manner. Variations in these parameters yield a minor effect when compared to the effect of the parameter under CO_2 injection itself (the displacement process and overriding effect due to the mobility ratio being 25). As mentioned previously, dynamic parameters were also constrained by the history match. If necessary, more work can be carried out by varying these parameters in the FFM to achieve a History Match. However, assessment of the impact in the simple box model did not show the necessity for this to be carried out at this stage in the project.

6. Capacity of Goldeneye hydrocarbon reservoir

As referred to in the Uncertainty Framework §5.1 the factors impacting CO_2 Storage Capacity are repeated in Figure 6-1 below. These are explained in the subsequent sections and linked to the uncertainty analysis in §5.

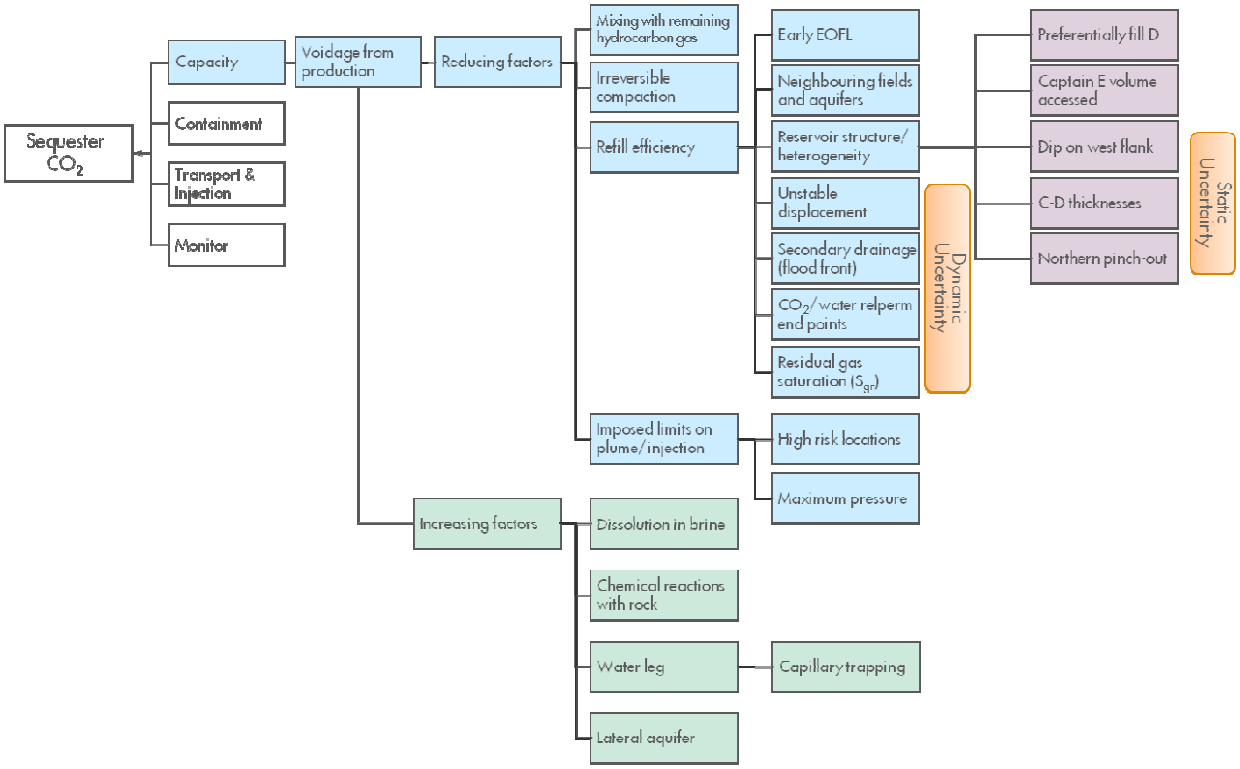

Figure 6-1. Factors impacting CO_2 Storage Capacity.

6.1. Total pore volume available: voidage from production

The total pore volume available for CO_2 was determined by making the assumption that all the pore volume vacated by produced hydrocarbons is replaced with CO_2 using the following factors:

- reservoir temperature of 83°C
- the characterised PVT properties of the Goldeneye fluids
- recharge to initial pressure at datum of 266 bara (3863 psia) at datum level of 2610m (8565 ft) true vertical depth subsea (TVDss)

This calculation gives a **storage capacity of 47 million tonnes of CO_2** using the total cumulative hydrocarbon production till cessation of production. This is twice as much storage capacity than that required for the Goldeneye CCS Demonstration Project. However, this is a maximum theoretical storage capacity assuming a perfect refill of the Goldeneye container. In reality there will be a series of additional factors, some of which will increase the storage capacity, and some which will reduce it. The following section analyses and describe these elements in order to determine an estimate for effective storage capacity.

6.2. Possible increases in the sequestration capacity

Permanent sequestration ("immobilisation") of CO_2 is achieved in time through various factors such as:

- structural and stratigraphic trapping
- dissolution of CO_2 into the formation brine
- residual CO_2 trapping
- chemical reactions of CO_2 with minerals present in the formation

The latter three processes increase the sequestration capacity and their significance grows with time. Of these, dissolution and residual trapping are discussed in some detail in the following sections.

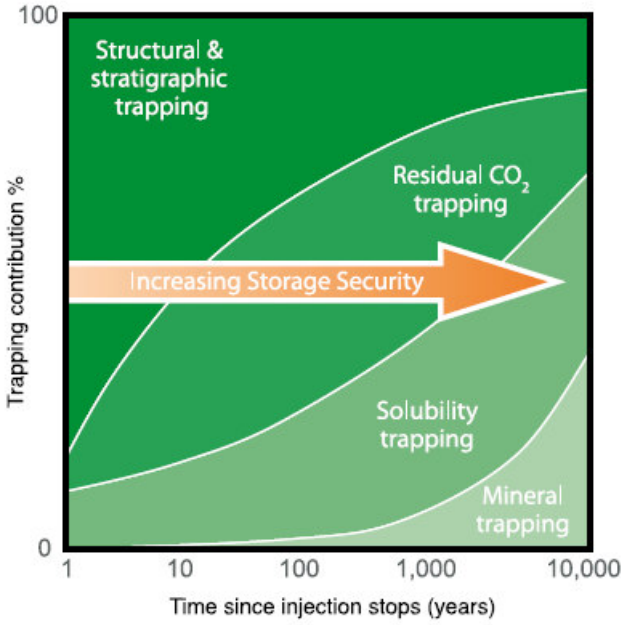

Figure 6-2. Storage security depends on a combination of different trapping mechanism. [4]

Mineralisation is strongly dependent on the geochemical composition of reservoir rock and happens over very long timescales. Over time, reactions with clay minerals will also lead to a removal of CO_2 from the gas phase. This effect has been modelled for this system and found to work over longer time scales than the injection period, as shown in the figure above. Therefore, it will not be taken into account for the storage capacity. Nevertheless, mineralisation will work in favour of the project reliability over a large period of time. For detailed results regarding this topic, refer to Geochemical Modelling Goldeneye Report. [5]

[4] Special Report on Carbon Dioxide Capture and Storage, 2005. Prepared by Working Group III of the Intergovernmental Panel on Climate Change [Metz, B., O. Davidson, H. C. de Coninck, M. Loos, and L. A. Meyer (eds.)]. Cambridge University Press, Cambridge, United Kingdom and New York, NY, USA, 442 pp, 2005.

[5] Geomechanical study into the competency of the reservoir and overburden of the Goldeneye field due to CO2 injection. Sietse de Vries and Ashok Shinde. Shell Projects & Technology Upstream. 2010.

6.2.1. CO_2 dissolution in brine

CO_2 solubility in water is higher than that of hydrocarbon gases such as methane, and is a function of pressure, temperature and water salinity. In general, CO_2 solubility increases with pressure and decreases with temperature. An increase in salinity of the reservoir water decreases CO_2 solubility significantly. Dissolution of CO_2 is an important immobilisation mechanism.

Several correlations are available from literature regarding CO_2 solubility. One of them was published by Chang, Coats and Nolen in 1996[6].

This correlation matches the solubility data of Wiebe[7] for liquid and supercritical CO_2 in water within ±10 scf/STB for temperatures between 54 °F and 212 °F and pressures up to 10000 psia. Above 212 °F the correlation can lead to unphysical behaviour.

The calculated solubility in distilled water can be adjusted further for the effects of salinity to obtain the solubility of CO_2 in brine.

Applying this methodology to estimate an average CO_2 solubility for the Goldeneye reservoir conditions (~3800 psi, 181 °F and 53.000 ppm of salinity) results in dissolution of 145 scf/bbl (7.7 kg/bbl, 4.6 % on weight). Goldeneye conditions are relatively favourable for CO_2 dissolution due to the low formation brine salinity.

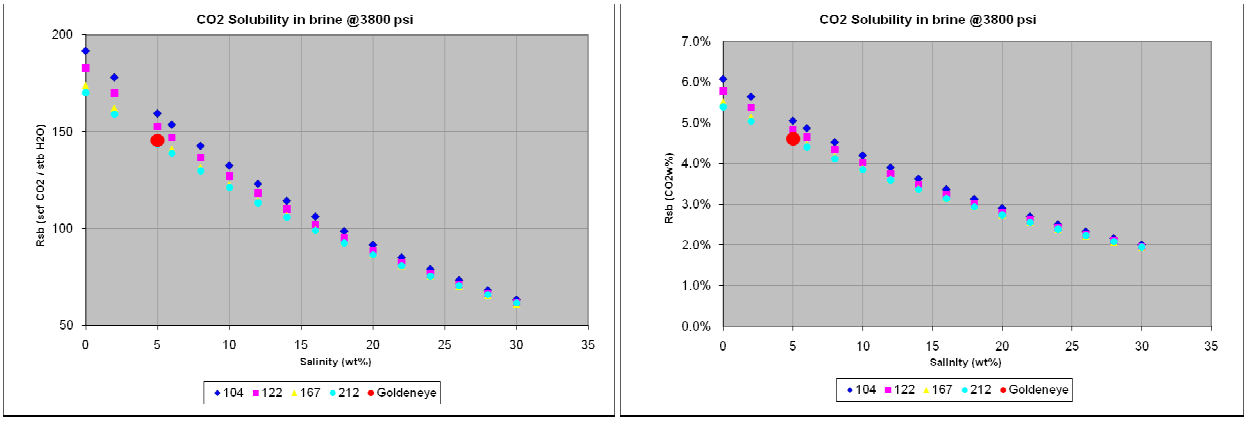

Figure 6-3. Calculated CO_2 solubility in NaCl brine at 3800 psi.

The increment in storage capacity has been estimated as 2.2%, taking into account a CO_2 solubility of 4.6% (weight) and that CO_2 will contact approximately 25% of the brine due to the nature of the displacement process (the remaining water saturation behind the CO_2 injection front is about 25%, estimated by fractional flow and Buckley-Leverett solution - see discussion in section 5.3.3.3).

6.2.2. Water leg and Lateral Regional Aquifer

Additional factors that could increase the storage capacity are related to the aquifer. The lateral regional aquifer surrounding Goldeneye is not part of the current analysis; nevertheless it represents a large opportunity for CO_2 aquifer storage. To the east of Goldeneye, the Captain sandstone extends approximately another 40-60 km and continues to deepen. To the west of Blake the formation starts to widen and eventually outcrops at the seabed about 50 km to the west of Blake. This situation may produce opportunities for further developments in the fairway and is under study by the Scottish Centre for Carbon Storage.

[6] Chang, Coats and Nolen 1996 "A Compositional Model for CO2 Floods Including CO2 Solubility in Water" SPE35164

[7] Wiebe, R.: "The Binary System Carbon Dioxide-Water Under Pressure," Chemical Reviews (1941) 29, 475.

On the other hand, there is also the possibility of increasing the storage capacity by considering the water leg beneath the Goldeneye structural trap. This is discussed in Section 7.3.3

6.3. Possible reductions in the pore volume available to the CO_2

Three effects were identified that reduce the vacated hydrocarbon pore volume available to CO_2:

- Mixing of the CO_2 and Goldeneye gas
- Irreversible compaction of the reservoir sands
- Efficiency of refilling:
    - Reservoir heterogeneities (Volumetric Sweep)
    - Unstable displacement (Dietz efficiency)
    - Water from the aquifer ingress that has become effectively immovable to CO_2 injection within the pores (Secondary drainage relative permeability effects – Water displacement)
    - CO_2/water relative permeability end points

Additionally, there are other elements (for example End of Field Life (EOFL) and the interaction with neighbouring fields), which could also impact the storage capacity. Nevertheless, if current conditions are maintained, no major impact is expected.

There may also be downside injection scenarios with high risk locations for injectors (although no such locations are currently identified) that could reduce capacity. These may include restrictions in maximum injection pressure in order to prevent fracturing the structural seal, or reservoir back pressure that could restrict the storage capacity. Nevertheless, current assessment indicates that these scenarios are unlikely.

6.3.1. Mixing the CO_2 and Goldeneye gas

Mixing of the CO_2 and the remaining hydrocarbon gas present in Goldeneye will have an impact on the CO_2 storage capacity estimation. CO_2 will be injected in a depleted predominantly methane gas reservoir. Due to the aquifer encroachment, there will be some residual hydrocarbon gas saturation (S_{gr}) in addition to the free gas saturation left in the top of the structure. Residual gas saturation has been estimated to be between of 25% and 38%, based on laboratory data. CO_2 will become mixed in, mobilising and displacing remaining hydrocarbons from the rock as in an Enhanced Gas Recovery (EGR) process. During this process CO_2 and Goldeneye gas will interact, and at reservoir conditions they will be miscible. The degree of mixing is unknown; however, the mixture will have a different density to that of pure CO_2.

By the time CO_2 is injected into the reservoir, part of the pore space will be filled with brine as a consequence of the aquifer ingression. During the process of CO_2 displacing brine, part of that brine will become effectively immovable due to secondary drainage relative permeability effects that will be discussed later in section 5.3.3.3. The time required to bring the system back to initial water saturation will be much longer than the injection period because there is insufficient time for gravity drainage to bring saturation into capillary equilibrium., This situation leaves an *"effective residual water saturation (S_{wr})"* behind the CO_2 front (just as a residual oil saturation to water is left in a normal waterflood) over and above S_{wi}, also because of reduced column thickness. It may be shown that the residual water saturation S_{wr}, could be around 25%, based upon fractional flow and Buckley-Leverett solution calculations.

If there is no mixing of CO_2 and hydrocarbon gas, 25% of the pore space will be filled with brine *("effective residual water saturation", S_{wr})* and another 25% will be filled with hydrocarbon gas (residual gas saturation, S_{gr}. This latter figure tends to be reduced to 20% due to gas compression when the reservoir is re-pressurised with CO_2 during injection). This leaves between 50-55% of pore space available for CO_2 storage. Nevertheless, an additional reduction of capacity is expected to occur once CO_2 eventually becomes mixed with the trapped hydrocarbon gas.

In order to evaluate this effect, the Real Gas theory was used. The equation has the following form:

$$pV = znRT$$

where, p = *absolute pressure, psia*

V = *volume, ft^3*

T = *absolute temperature,* °R

n = *number of moles of gas, lb-mole*

R = *the universal gas constant which, for the above units, has the value 10.730 psia ft^3 / lb-mole* °R

z = *gas compressibility factor z is a dimensionless quantity and is defined as the ratio of the actual volume of n-moles of gas at T and p to the ideal volume of the same number of moles at the same T and p*

By understanding the variation of the compressibility factor z at different concentrations of mole percentage of CO_2 and hydrocarbon gas (mainly methane), we can estimate the capacity reduction from the mixing effect as a function of the actual moles of CO_2 in an ideal mixing scenario, compared with a no mixing theoretical scenario.

Based on this approach, the reduction in capacity has been estimated to be as much as 6%. This assumes 100% mixing between CO_2 and the remaining hydrocarbon gas; however simulation has shown that instead of a perfect mix, a hydrocarbon gas bank is formed at the tip of the plume. This results in imperfect mixing and hence the reduction will be smaller than 6%, (i.e. classifying it as a small reduction factor).

6.3.2. Irreversible compaction of the reservoir sands

The reservoir is currently grain supported, therefore compaction is minimal. Additionally, the depletion during hydrocarbon production is forecast to be from ~263bara to ~138bara (~3815 psi – 2000 psi). Irreversible compaction is expected to be minimal.

When CO_2 is injected in the Captain sandstone, the small amount of calcite in/around the pores will be dissolved. However, there is not much carbonate cement in the reservoir parts that will be used for the CO_2 injection. So, the pore space will increase a small amount (greater volumetric injection will be available) and the matrix will become slightly weaker, although the risk of pore collapse is avoided.

Compaction experiments carried out in 1998-1999 showed that the compaction of cores from Goldeneye sands is partly elastic (i.e. reversible) and partly plastic (i.e. irreversible). Results from the experiments showed minimal compaction, and the porosity change was about 0.3%. As a result this effect can be considered to have negligible impact. For further details regarding this topic, refer to Goldeneye Geomechanical Report[8].

[8] Goldeneye Geomechanical Report. 2010

6.3.3. Efficiency of refilling

Refill efficiency has been divided into macroscopic and microscopic fill efficiency. The microscopic efficiency has been partially discussed under the last point above, but macroscopic efficiency also includes the impacts of permeability variations in the subterranean formation and dynamic stability of the flood fronts due to mobility ratio (viscosity and relative permeability).

6.3.3.1. Reservoir heterogeneities

Reservoir heterogeneities are highlighted in Goldeneye by the permeability contrast with the Captain D sand. This sand contained ~78% of the original hydrocarbon (Figure 6-4). Injected CO_2 will tend to follow the path of least resistance. Full field simulation has confirmed that, during the injection phase, the CO_2 preferentially fills and follows the D sand. If only the D-sand was available for filling, the storage capacity would be reduced by **9.7 million tonnes CO_2**.

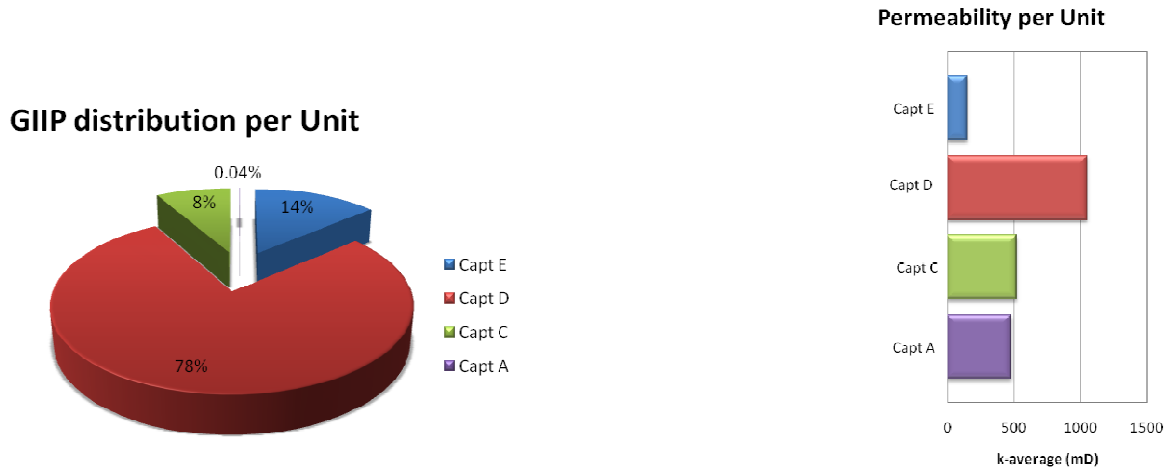

Figure 6-4. Goldeneye GIIP distribution and average permeability per geological unit.

After injection, buoyancy forces dominate, and the CO_2 contracts back into the original gas cap. It also begins to fill the overlying Captain E sand. The Captain E sand accounts for a further 13.7% of the original hydrocarbons in place and could potentially add an additional 3.4 million tonnes CO_2 if 100% refilling efficiency is considered (based on an estimated gas ultimate recovery of 60 Bscf). However, part of it will be filled with the remaining undeveloped hydrocarbon gas, and when the effects of some of the reducing factors that affect the Captain D unit are taken into account, just a part of Captain E will be finally flooded with CO_2 (mainly the bottom part). Furthermore, this will occur after injection ceases, and it could take a long time for the buoyancy forces to overcome the capillary forces and slowly fill the Captain E sand. Numerical simulation results show that only **1.3 Mt of CO_2** makes its way into Captain E, 20 years after injection stops.

6.3.3.2. Unstable displacement

The effects of unstable displacement during CO_2 injection process in Goldeneye could potentially reduce the short term (i.e. during injection) storage capacity.

As a consequence, a simulation model was constructed to investigate these effects. A dipping box simulacrum model representing roughly one quarter of Goldeneye in volume, with similar rock properties (permeability and porosity) and dip angle was used to simulate these effects. The model was conditioned with a 10 year depletion period, a further 10 years of recharge from the aquifer and finally, a 10 year CO_2 injection period.

Phase behaviour was represented using a Peng Robinson 1978[9] equation of state (EoS), calibrated to match the Goldeneye hydrocarbon fluid description from GYA03, CO_2 properties (density and viscosity) at reservoir conditions[10] and CO_2 dissolution in brine.

Sensitivities were carried out on a range of values of effective water relative permeability at residual gas saturation (S_{gr} = 30%) within the observed data, varying between 0.1, 0.25 and 0.6.

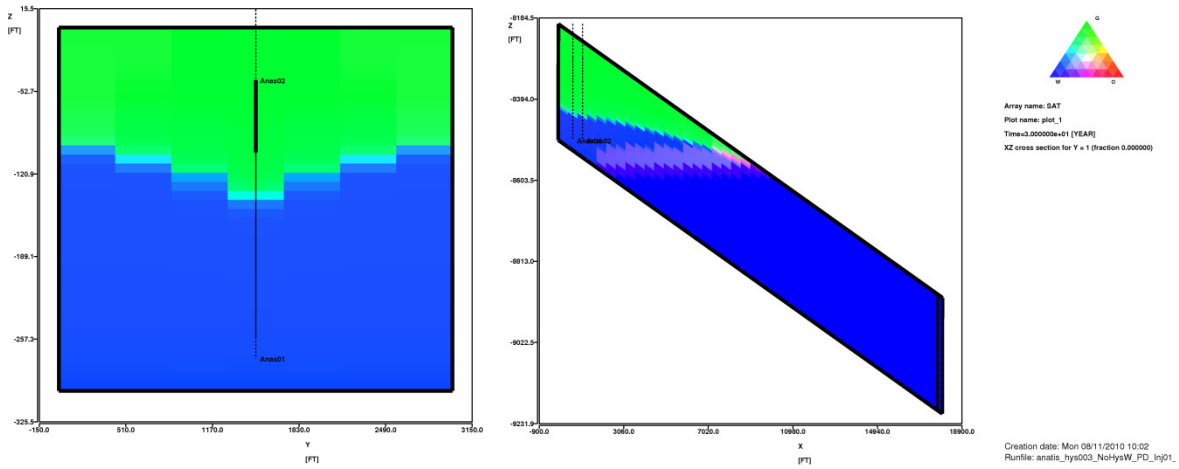

Figure 6-5. Cross section in ternary diagram. Sensitivity with krw = 0.6 @ S_{gr} = 0.30.

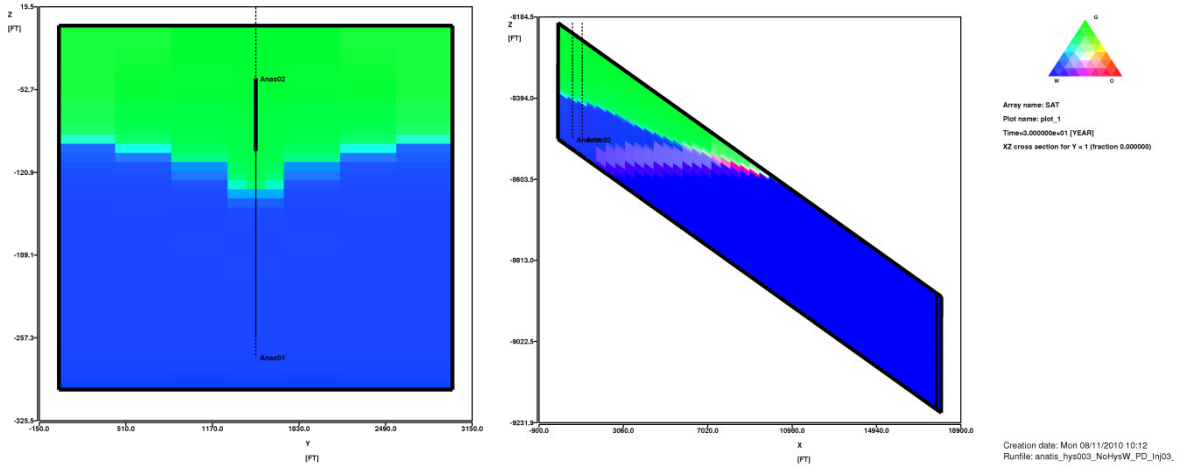

Figure 6-6. Cross section in ternary diagram. Sensitivity with krw = 0.25 @ S_{gr} = 0.30.

[9] Peneloux, A., E. Rauzy., and R. Freze. "A Consistent Correction for Redlich-Kwong-Soave Volumes". Fluid Phase Eq. 8, 7-27 (1982).

[10] PVT Modelling Report for CO2 in Goldeneye Project. Doc No. OP200D3 (RT 082). 2181-18-PT-PX-0504-00001

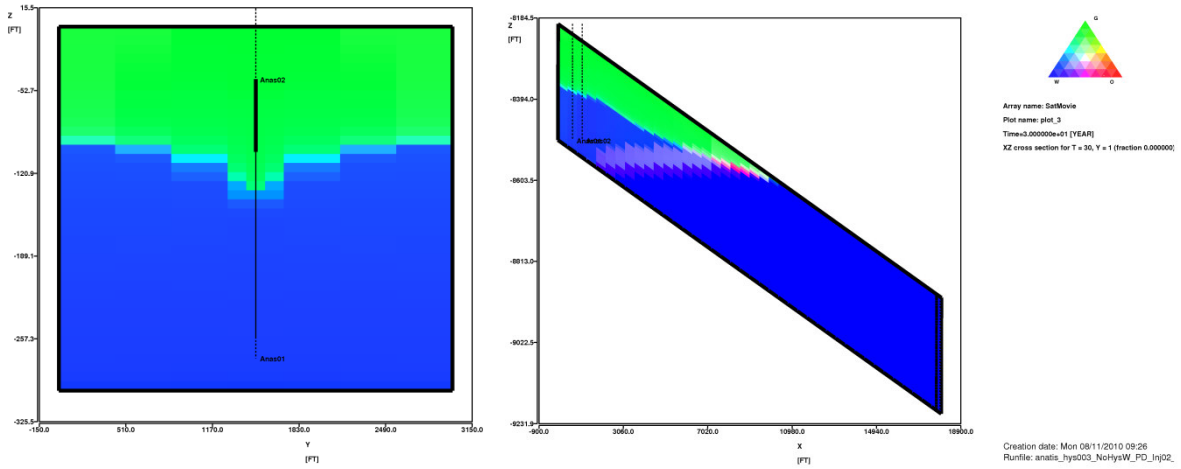

Figure 6-7. Cross section in ternary diagram. Sensitivity with krw = 0.10 @ S_{gr} = 0.30.

Results from the model confirmed that a strong override of water by CO_2 will occur in the reservoir, producing a CO_2 tongue moving downwards due to the unstable displacement (a consequence of the unfavourable mobility ratio). As expected, the tonguing effect is enhanced in proportion to minimisation of the water relative permeability end point, creating a Dietz tongue that could be almost parallel to the top of the interval. This means that, during injection, the mobile CO_2 dense phase can extend below the original hydrocarbon water contact.

The simulacrum models show the impact of the water relative permeability endpoint on the Dietz tongue within the original hydrocarbon column, with the dip of the plume approaching the reservoir dip as the relative permeability reduces. However, once the plume has moved beyond the OWC the impact of trapped gas on water relative permeability is reduced, because the gas plume is then displacing 100% brine in the aquifer.

Finally, the refill efficiency is highly impacted. Probably less than 50% of Captain D will be flooded with CO_2 (in the vertical sense) before the CO_2 has moved under the original OWC, tonguing preferentially into the water leg beneath the reservoir. However, this is a short term effect that will happen only during injection. The Dietz tonguing behaviour means that the tip of the CO_2 plume will reach the original OWC after injecting just the first 10 to 12 million tonnes of CO_2, but the structure will continue to fill until the total 20 Mt have been injected.

6.3.3.3. Secondary Drainage Relative Permeability

The secondary drainage relative permeability curve is expected to follow the primary drainage curve, However, the time required to bring back initial water saturation will be much longer than the injection period because there is insufficient time for gravity drainage to bring saturations into capillary equilibrium.

In order to estimate how large the effective "residual water saturation" (S_{wr}) left behind the CO_2 flood front could be, both analytical and numerical estimations were carried out. Buckley-Leverett displacement theory and fractional flow equations were applied for a process where gas (CO_2) is displacing water. Sensitivity analysis was carried out within the water relative permeability Corey Exponent.

Fractional flow analysis allows calculation of the average saturation of the displacing front (CO_2) and hence, the complemented displaced phase (in this case brine). Numerical simulation results have

shown that an unstable gravity dominated displacement will occur in Goldeneye. Therefore the fractional flow analysis was carried out incorporating a gravity element, in order to take into account the gravity forces in addition to the viscous displacement.

A set of relative permeability curves as well as rock properties were used taking into account Goldeneye basic data from logs and SCAL analysis available at the time These included: S_{wi}, porosity, NTG, vertical permeability and thickness, among others. Corey exponents were used as sensitivity and CO_2 and brine properties were taken at Goldeneye reservoir conditions.

The average water saturation left behind once CO_2 injection has occurred can provide insight into the physics represented in the simulation model.

The following figures show the results of both Buckley–Leverett and fractional flow analytical calculation, as well as the numerical results from a simple box model in MoReS already described in the previous section.

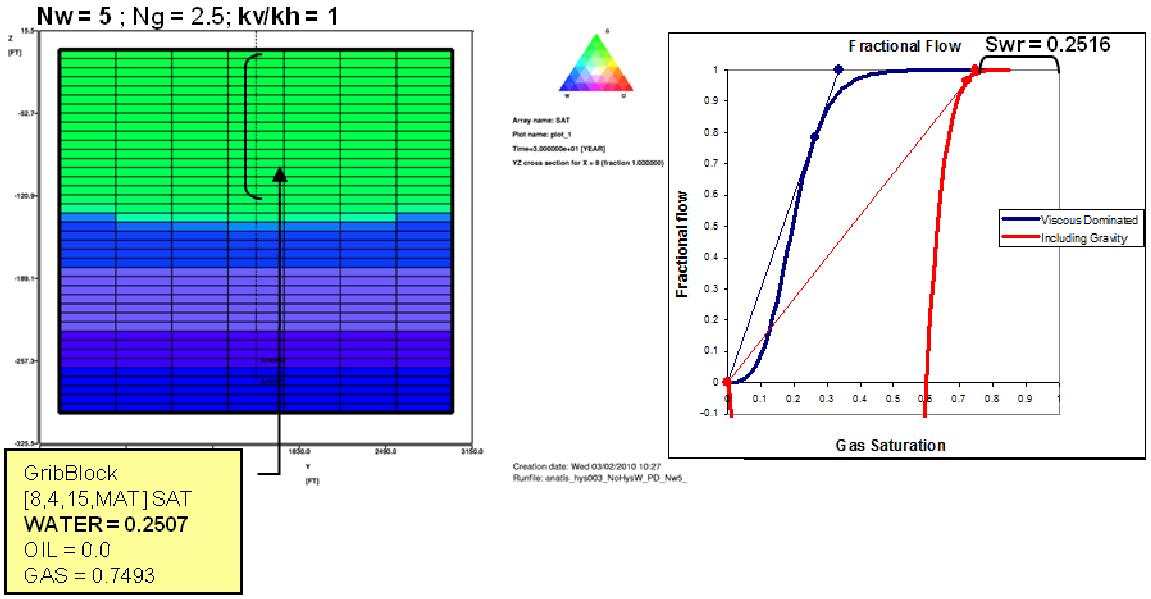

Figure 6-8. Cross section vs. fractional flow curve with B-L solution. Nw = 5.0.

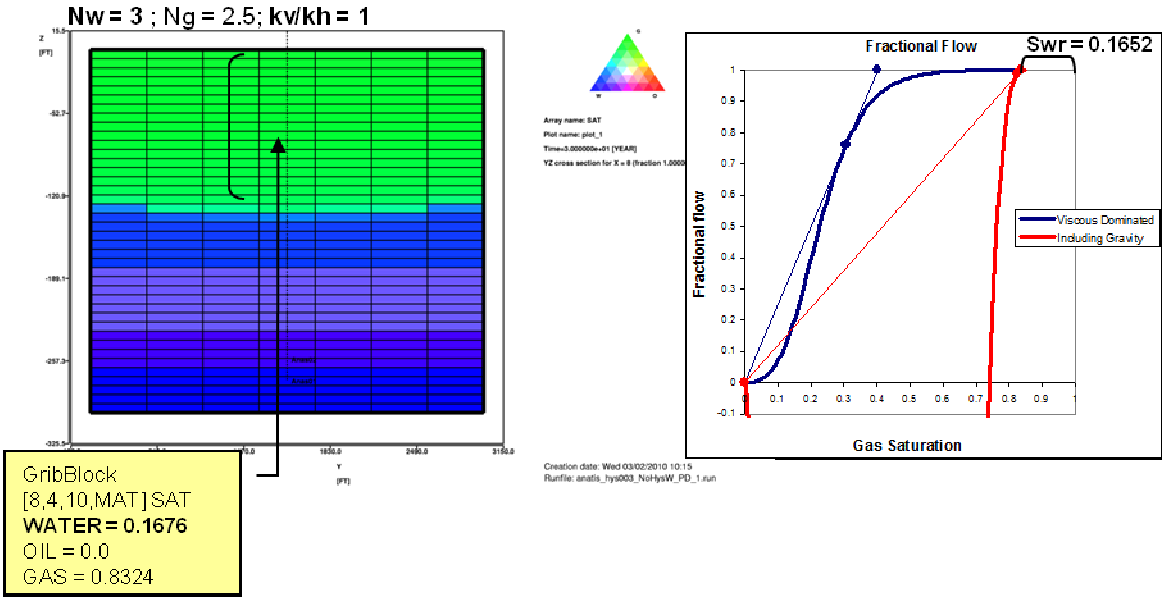

Figure 6-9. Cross section vs. fractional flow curve with B-L solution. Nw = 3.0.

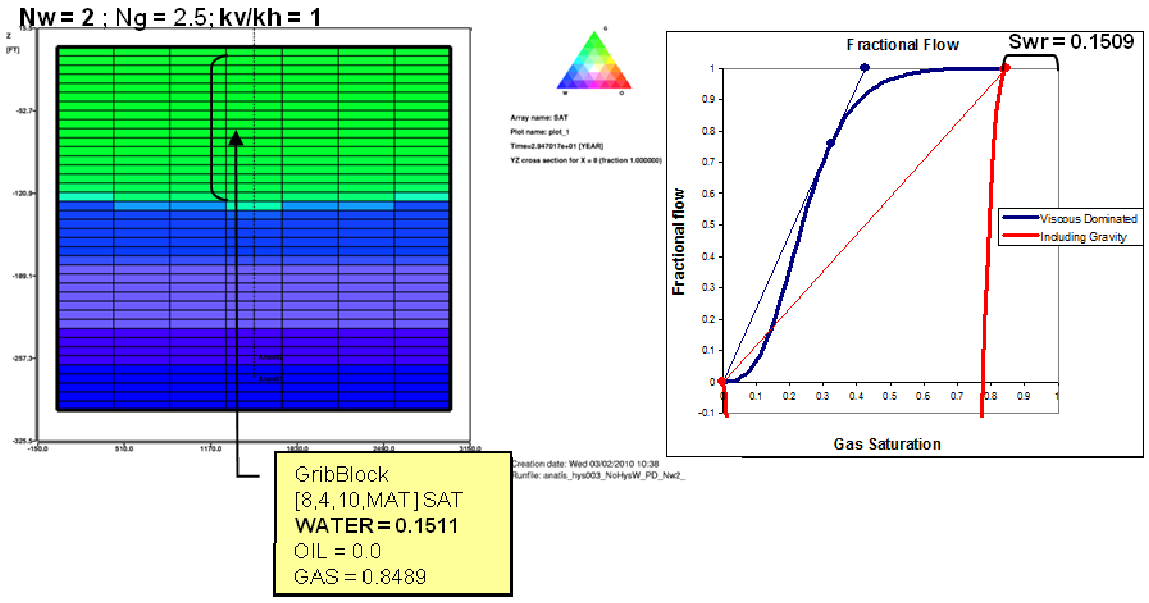

Figure 6-10. Cross section vs. fractional flow curve with B-L solution. Nw = 2.0.

The cross sections and fractional flow numbers agree, meaning that the physics represented in the numerical model are performing as expected. This traditional fractional flow curve combined with the Buckley - Leverett solution gives the average saturation behind the injection front. In this case, that will be the average CO_2 saturation within the plume, and as a consequence, the complement will be the average water saturation (Sw_{avg}) left behind the injection front. It may be observed that for a range of Corey exponents of 2, 3 and 5, Sw_{avg} can vary from 0.15 to 0.25, depending on how easy it is to displace the water during CO_2 injection. Based on literature and the unfavourable mobility ratio expected for the reservoir, a Corey exponent of 5 could be the more appropriate figure. This yields a higher water saturation left behind the injection front, considerably higher than the connate water saturation observed in Goldeneye (S_{wi} ~ 0.07). Accordingly, this factor represents an important storage capacity reduction element for Goldeneye, because it, in conjunction with S_{gr}, will reduce the pore space available.

6.3.3.4. CO_2/water relative permeability end points

The injection rate can vary significantly for different relative permeability values and injectivity could also be sensitive also to variables that define the relative permeability curves. In addition, the end point of the relative permeability curves is conditioned to the mobility ratio (M) of the fluids, and has a large impact on the CO_2 plume shape. As previously mentioned, water will be by-passed and gas tongues will develop, leading to an unfavourable displacement. In such conditions, the CO_2 plume will travel further away from the injection point, diminishing the average CO_2 storage density and requiring a larger volume for storage[11]. As a consequence, a proper assessment of the relative permeability variables is important for the refill efficiency of the system.

One of the challenges of properly modelling CO_2 injection is that relatively little is known about relative permeability end points of a CO_2/water system. Most published work refers to instances in Van Genuchten or the Brooks and Corey model[12]. Yet until recently, no relevant data has been published regarding relative permeability and capillary pressure of CO_2/Brine systems at in situ conditions. One of the studies available is that by Bennion and Bachu[13,14] reporting a series of laboratory measurements performed in the Western Canada sedimentary basin on six samples of carbonates and sandstones. These plugs all have low average permeability (sandstone samples with permeability 0.55, 2.2 and 5.78 mD, and porosity of 11.7 %, 12.6 % and 12.5 %), and are not thought to be representative for good quality reservoirs like Goldeneye. The relative permeability end point for CO_2 measured at irreducible water saturation varied around 0.55, 0.12 and 0.33, respectively. No in-situ saturation monitoring (e.g. by imaging) was used, and no in-situ saturation profiles in the sample were available. The CO_2 endpoint relative permeability and the capillary end effect were determined by multi-rate end point floods.

Alternatively, Stanford University[15] also published the results of a study regarding physical modelling of CO_2 sequestration regarding relative permeability of CO_2/Brine system done using a Berea sandstone core with a porosity of 0.23 and permeability of 885 mD (very similar to Goldeneye rock). Results show that CO_2 dissolution and evolution have very significant effects on the displacement of water by gas injection. Again the gas relative permeability end point was in the neighbourhood of 0.2, implying a reduced mobility of CO_2 in the presence of brine.

Alternative schools of thought express the idea that the relative permeability of CO_2/Brine should not be that dissimilar to that found in conventional experiments conducted with brine and a model fluid (i.e. decane).

This could have an impact in both injectivity and CO_2 displacement, therefore more work has to be carried out in order to corroborate this assumption. As part of the Goldeneye project, a SCAL program was assembled to analyse the most important variables impacting displacement, via direct measurement of Goldeneye reservoir rock with a CO_2 /Brine system,:

- Trapped gas saturation to brine and end point relative permeability
    - Determines mobility ratio of displacement of aquifer brine by injected CO_2

---

[11] L.P. Dake, 1978: "Fundamentals of Reservoir Engineering", Elsevier 1978

[12] J.M. Schembre-McCabe (SPE), J. Kamath (Chevron Energy Technology Company), R. Gurton (Chevron Australia), 2007: "Mechanistic Studies of CO_2 Sequestration", IPTC 11391

[13] B Bennion, S Bachu, 2005: "Relative permeability characteristic for supercritical CO2 displacing water in a variety of potential sequestration zones in the Western Canada sedimentary basin". SPE95547

[14] B. Bennion and S. Bachu, 2008: "Drainage and imbibition relative permeability relationships for supercritical CO2/brine and H2S/brine systems in intergranular sandstone, carbonate, shale, and anhydrite rocks". SPE 99326:1–13.

[15] Roland N. Horne, 2008. "Physical Modelling of CO_2 sequestration". Stanford University. Department of Energy Resources Engineering. CEC-500-2007-113

- Limits lateral migration of plume in aquifer by capillary trapping of CO_2
- CO_2 relative permeability in the plume at water saturations in range 25 to 35%

The SCAL programme was designed specifically for Goldeneye conditions and plume geometry:

- Combination of ambient (air/brine) and reservoir condition (CO_2/brine) tests
- Special procedures to reduce issues over component exchange between CO_2/brine
- May generate one of the first reliable published data sets

The main impact of the CO_2/water relative permeability end points on the storage capacity is related to the displacement mechanism, affecting the behaviour of the Dietz tongue and potentially generating scenarios where the CO_2 can move to levels below the original OWC. From there it could eventually migrate under the spill point. As a result, it is difficult to assign a specific reduction factor to it. Addressing the direct impact of end point relative permeability on the refilling efficiency (based on how unstable the displacement is, i.e. extent of the Dietz tongue), will give an approximation of the storage capacity reduction.

Sensitivities were carried out in the dipping box model, for a range of values of effective gas (CO_2) relative permeability (k_{rg}) at residual water saturation, of 0.8, 0.5 and 0.25. The following figures show the results.

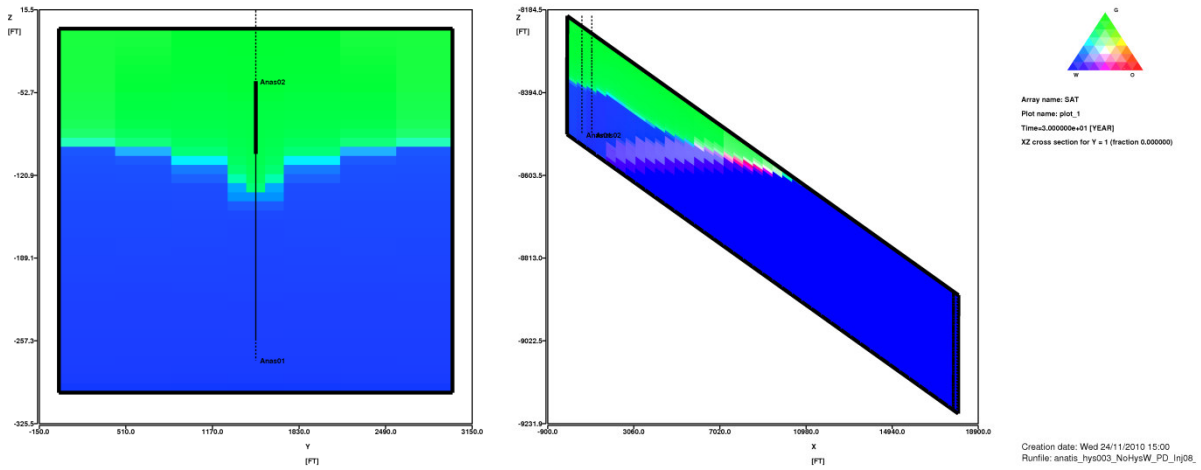

Figure 6-11. Cross section in ternary diagram. Sensitivity with k_{rg} = 0.8.

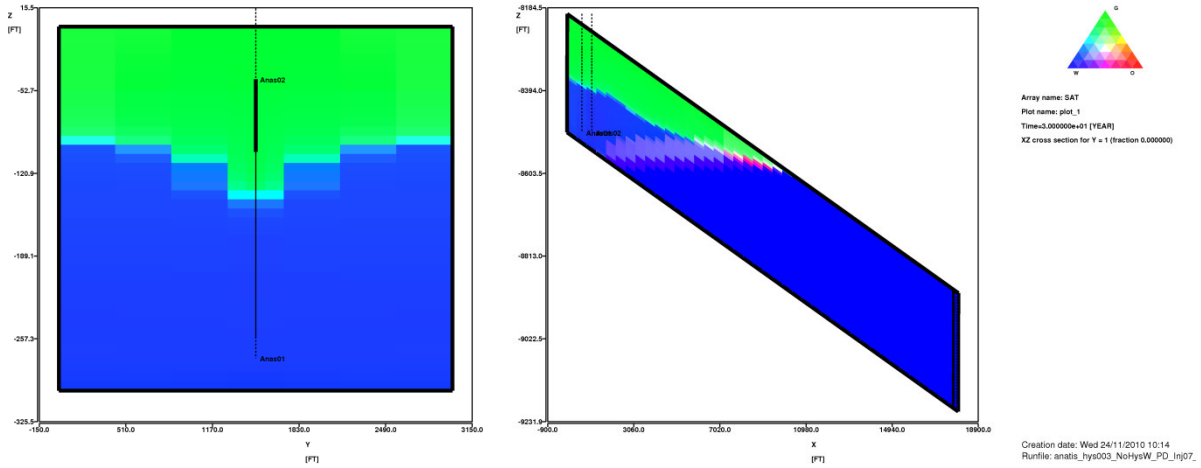

Figure 6-12. Cross section in ternary diagram. Sensitivity with krg = 0.50.

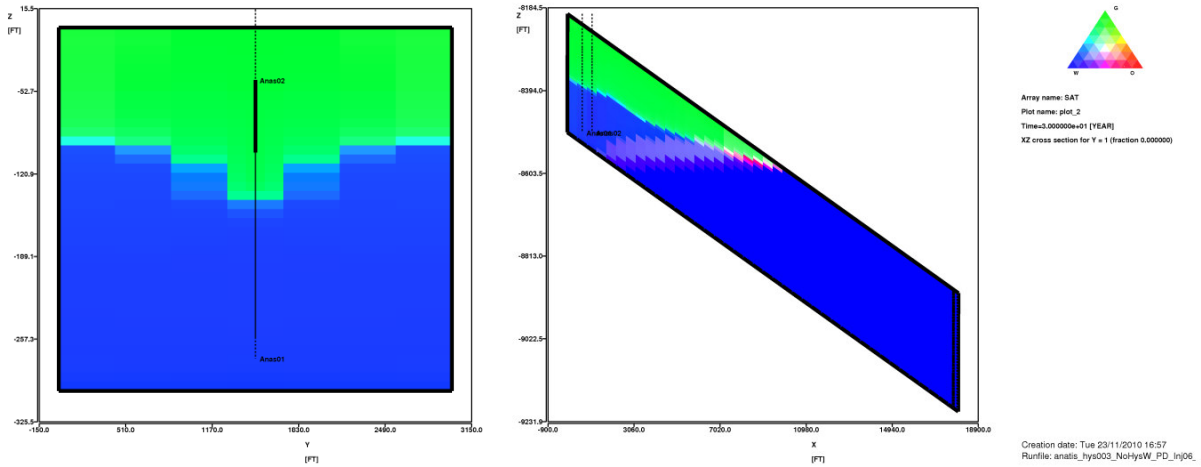

Figure 6-13. Cross section in ternary diagram. Sensitivity with krg = 0.25.

As may be seen, the relative permeability end points have a minor impact on the displacement, making the plume go slightly further in the case where k_{rg} = 0.80 meaning that it will move easily, and the other way round when k_{rg} is restricted (as mentioned above by different publications) to lower values like 0.25.

However, a bigger effect will be seen in injectivity, where the overpressure needed could be higher than expected. This topic will be discussed in detail in a separate report[16].

[16] Injectivity Analysis Preparation. Doc No. SP-PT040D3

6.4. Geological Carbon Storage Capacity of Goldeneye

Considering both increasing and reducing factors, the effective storage capacity can be estimated as a function of available volume (production-based) and refill efficiencies based upon the most important reducing and increasing factors mentioned above, which are later multiplied together.

$St_{Capacity}$ = *Available Volume * Volumetric Sweep * Dietz efficiency * Water displacement *Mixing * Dissolution*

where,

- Available volume: total pore volume available production-based.
- Volumetric sweep: considering where the CO_2 will preferentially go in based on reservoir quality (heterogeneities).
- Dietz efficiency: related to the unstable displacement of CO_2 displacing water under a unfavourable mobility ratio
- Water displacement: "residual water saturation" (S_{wr}) left behind the CO_2 flood front
- Mixing: of CO_2 with remaining hydrocarbon gas saturation (undeveloped + trapped)
- Dissolution: of the CO_2 in both the pore water and the underlying aquifer.

Mineralisation has been identified as a potential increasing factor (Section 6.2), but it makes significant contributions over timescales long after the injection period has finished. It is therefore not considered further here. Other factors, such as irreversible compaction (Section 6.3.2), are considered negligible.

Additionally, processes such as the possible filling of Captain E sand when buoyancy forces dominate after cessation of injection may be added at the end of the capacity estimation.

It is important to highlight that the unstable displacement factor (Dietz efficiency) will be in play only during injection, and will determine the point in time when the tip of the CO_2 plume reaches the boundary of the OOWC. Thereafter, CO_2 will continue to spread inside the CO_2 storage complex.

In addition to the storage capacity defined by the structural trap of Goldeneye, the water leg beneath the reservoir that lies within the storage site, could potentially add some extra capacity, based on numerical simulation results.

Finally, an areal sweep efficiency will exist that should also be taken into account. This will be difficult to analytically estimate due to the non uniform shape of the CO_2 plume, but it will be evident in the numerical simulation results.

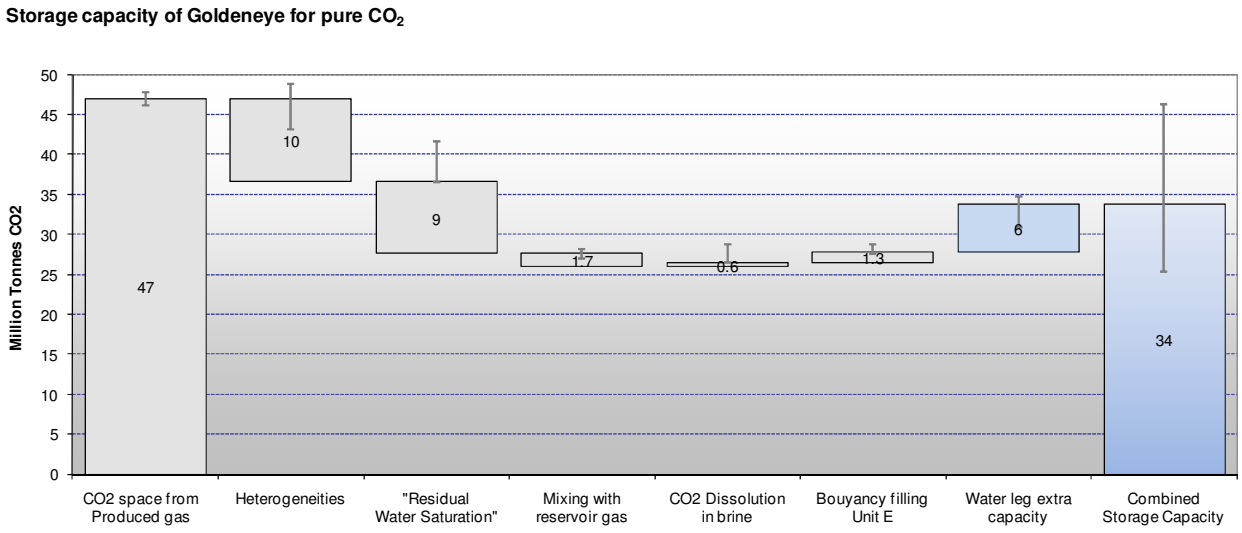

Figure 6-14. Post-injection effective storage capacity of Goldeneye

Using this equation and taking into account the additional capacity of the original water leg beneath the field and inside the storage site, Goldeneye's effective, post-injection and combined geological carbon storage capacity can be estimated as **34 million tonnes of CO_2**, which is more than adequate to store the 20 million tonnes intended.

The uncertainty bars in each of the elements of Figure 6-14 represents the uncertainty observed.

- **Heterogeneities:** reservoir heterogeneities were highlighted in Goldeneye by the permeability contrast with Captain D sand and the assumption that most if not all of the CO_2 will be injected in Unit D. This sand contained ~ 78% of the original hydrocarbon, however, this factor has a range among all the geologic realisations available for Goldeneye, that ranges from 70% to 82% and consequently this uncertainty bar represents that span.
- **Residual water saturation:** The size of the effective "residual water saturation" (S_{wr}) factor left behind the CO_2 flood front, was estimated by Buckley-Leverett displacement theory and fractional flow equations. S_{wr} ranged from 15% to 25% and this uncertainty bar represents that span.
- **Mixing with hydrocarbon gas:** the reduction in capacity was estimated to be as much as 6%. This is assuming 100% mixing between CO_2 and the remaining hydrocarbon gas, however, simulation has shown that instead of a perfect mix, a hydrocarbon gas bank is formed at the tip of the plume, meaning that mixing is not perfect. As a consequence the reduction will be smaller than 6%, making it a small reduction factor. 4% was taken as a lower end for this element, which is a relatively small figure over-all.
- **CO_2 dissolution in brine:** the increment of storage capacity was estimated as 2.2%, taking into account a CO_2 solubility of 4.6% (weight) and that CO_2 will contact approximately 25% of the brine due to the water saturation left behind the CO_2 injection front. Nevertheless, dissolution is considerably more complicated than the obviously instantaneous dissolution described before. In addition there will be diffusion of the CO_2 dissolved in the water, allowing more CO_2 from the gas phase to dissolve in the aqueous phase. There will also be a convective mixing effect, because the density of water saturated with CO_2 is greater than that of undersaturated water, hence density instability is created and eventually plumes of CO_2 laden water flow downwards through the formation. Assuming this, a maximum dissolution reduction was calculated to be 11.2% assuming not only the height of the CO_2 plume (residual water saturation) is contacted but in the long term the whole reservoir thickness.
- **Buoyancy filling of Unit E:** after injection, buoyancy forces dominate, the CO_2 contracts back into the original gas cap, and it also begins to fill the overlying Captain E sand. It was seen in simulation that Captain E will eventually be flooded with CO_2 but mainly only the bottom part. A refilling efficiency for Unit E of between 33% and 66% was assumed in order to create the span for this uncertainty bar.
- **Water leg extra capacity:** in this case the bar shows an uncertainty margin dominated by the static uncertainties regarding the structural west flank of the field. The alternative realisation SMR3.05 (shallower west flank) allowed only 3 Mt of CO_2 to be stored in the water leg, while SMR3.15 (pinch-out sensitivity) allowed 7 Mt and the reference case (SRM3.1) 6 Mt.

In contrast to a traditional E&P approach (where a probabilistic distribution will define a P10-P50-P90), in a sequestration project capacity must be demonstrated at P0 or near certainty. The summation of all the positive and negative uncertainty bars gives the total uncertainty range for the storage capacity at the end of injection. The extremes represent the unlikely scenarios where all the elements decreasing or increasing the storage capacity all happen in the downside or upside cases.

The final capacity and the extremes are for the specific injection pattern using the current Goldeneye well penetrations and currently proposed store rock volume. If for example, more CO_2 were to be

injected, an alternative pattern with new penetrations could yield a higher post injection capacity by forcing more CO_2 to be stored in the water leg.

Nevertheless, this approach still results in a storage capacity that sits above the 20 Mt mandated by the UK CCS Demonstration Project, depicting a lower end scenario of about 25 Mt.

7. Full field modelling

The analytical calculations discussed above show in the base case that there is about **8 million tonnes of spare capacity** inside the original hydrocarbon gas field, which is sufficient to allow for additional discounting effects, without including the additional storage capacity of the water leg.

Full field dynamic modelling of the system was undertaken to check that the interaction of the geological system and the dynamic system did not produce effects that reduced the capacity. The dynamic models are based on three 3D geological realisations (Section 5.2) and include all the discount elements previously mentioned (Section 6.3). The models have confirmed the applicability of the analytical calculations.

The modelling is described below.

7.1. Final production phase

The model was matched to historical production data to July 2010. The model was run on after this date to 1.1.2013, with the remaining producing wells (GYA01 and GYA02S1) constrained by tubing head pressure. The simulated end of field life was between November 2010 and January 2011 in the three models[17].

Table 7-1. End of production life in different models

Geological model	GYA01	GYA02S1
FFM 3.1	December 2010	November 2010
FFM 3.05	December 2010	January 2011
FFM 3.15	November 2010	January 2011

7.2. Injection wells

The target for CO_2 injection is 20 Mt CO_2 in a period of between 10 and 15 years starting at the end of 2014/beginning of 2015. In order to make best use of existing resources all CO_2 injection is planned to be via the existing wells, which will be converted from production to injection service. In the model no changes have been made to the completions of the wells. For the initial sensitivity work, the flow of CO_2 into the wells is governed by injection tables, designed to represent 4½ inch completion tubing. The high permeability of the reservoir means that the capacity results are insensitive to minor variations in the completion characteristics of the wells. This was additionally verified by running a scenario, using data for the planned completions (Well completions Section 7.4).

[17] These forecasts were made in Q3 2010. Since the forecasts were made the field has been observed to cut water in GYA01 and GYA02S1 at dates similar to those in FFM 3.1.

CO_2 injection is modelled from 1st December 2014, with only two wells operating at a low initial rate – assumed here as 0.25 Mt CO_2/year. The requirement for a low initial injection rate comes from the CO_2 source at Longannet. It is expected that initially only one of the two carbon capture plants will be operating, with the second brought on-stream after six months. The details of the commissioning process will be revisited for detailed design in the simulation model. The low injection rate continues for six months – by which time 0.25 Mt CO_2 has been injected. At this point (1st June 2015), the remaining wells (as required for the scenario) come on-stream and all wells operate at the same maximum injection rate, such that the remaining 19.75 Mt can be injected in the next 9.5 years. For the simulation work here, 10 years is assumed for the maximum duration of the injection phase. In some cases, testing specific sensitivities, the rates are permitted to be higher, or the injection continued for a longer period of time.

In all cases, the wells are further constrained by a maximum BHP when injecting. For the initial simulation work, this has been set as 4000psi at datum of 8400ft [2560.3m] TVDSS. It is recognised that the pressure immediately around the wellbore will be higher than that further away. For the purposes of reporting the results the datum corrected average pressure for gas (hydrocarbon and CO_2) in the Captain D is used.

7.3. Injection scenarios

Several injection scenarios were modelled to test the storage margin referred to above in Section 6.4. In each case, the maximum reservoir pressure (after injection) and the total mass of CO_2 injected are determined. Also, the extent of the CO_2 plume (with respect to the location of the structural spill point) is checked. The aim is to establish that it is possible to inject 20 million tons of CO_2 in 10 years, without risk of egression from the store.

a) **Base case**: injection pattern as described above. GYA03 is not used for injection in this scenario, being kept in reserve and used as a monitoring well.
b) **Maximum available storage (1):** inject into the four base case wells (GYA01, GYA02S1, GYA04 and GYA05) at double the rates in (a). Check the injected volume required to cause an egression from the store or to exceed initial (pre-production) average reservoir pressure.
c) **Maximum available storage (2):** continue base case injection (case a) at same rate and in same wells as in case (a), for an extended period (to year 2075). Check the injected volume required to cause an egression from the store or to exceed initial (pre-production) average reservoir pressure.
d) **Failure of one injector**: rates as above, but after 5 years, one of the four wells fails and is replaced immediately with well GYA03 injecting at the same rate.
e) **Test risk of egress over the western and eastern flanks of the field:** inject the same total rates as above, but equally divided between only wells GYA02S1 and GYA04 (eastern wells) or GYA03 and GYA05 (western wells).
f) **Worst case of well availability**: attempt to inject the entire target CO_2 into one well only.

All scenarios were run in each of the three geological realisations – 3.1 (reference case), 3.15 (northern pinch-out sensitivity) and 3.05 (west flank sensitivity).

The key points to note for each scenario are:

- Total mass of CO_2 which was injected
- Extent of CO_2 plume outside the original hydrocarbon/water contact, at the end of injection

- Average reservoir pressure for gas in Unit D (the main storage unit)

A total of 14 scenarios were run, in each of the three models. Results are given in Table 7-2 to Table 7-4.

The data in the tables is as follows:

- CO_2 injected: the mass of CO_2, in millions of tons, delivered by all wells, in period 2015 to 2025. One exception to this is for the case "Inject to 2075", where injection continues at the same rate until year 2075.
- Injected CO_2 in the Original Gas Zone: CO_2 resident, immediately after cessation of injection (1st January 2025) within the original gas/oil contact.
- Final average Unit D pressure: the pressure averaged over the gas zone in Captain D, immediately after cessation of injection (1st January 2025).
- Plume extent beyond original OWC on 1st January 2025 – to both east and west of field: approximate distance from OOWC to the tip of the CO_2 plume, at top Captain D. This estimate is limited by the granularity of the dynamic model – the gridblocks are 100m x 100m areally. A positive number here means that the plume extends outside the OOWC, negative means it lies within the contact.

Table 7-2. Storage capacity results. Summary table for FFM 3.1 (reference case)

FFM 3.1	CO_2 injected (Mt)	Injected CO_2 in original gas zone (Mt)	% CO_2 outside original OWC after injection	Plume extent beyond original OWC –west (m)	Plume extent beyond original OWC –east (m)
Base case	**20**	**18**	**13%**	**700**	**0**
GYA03 and GYA05	20	16	**21%**	800	-1500
GYA02S1 and GYA04	20	18	**9%**	-1000	300
GYA01 failure	20	17	**12%**	600	0
All in well GYA01	14	13	**3%**	200	-1300
Double rate	29	22	**25%**	1400	600
Inject to 2075	68	38	**45%**	1000	500

Table 7-3. Storage capacity results. Summary table for FFM 3.05 (west flank sensitivity)

FFM 3.05	CO_2 injected (Mt)	Injected CO_2 in original	% CO_2 outside	Plume extent	Plume extent

		gas zone (Mt)	original OWC after injection	beyond original OWC –west (m)	beyond original OWC –east (m)
Base case	**20**	**18**	**10%**	**600**	**-100**
GYA03 and GYA05	20	16	**18%**	600	-800
GYA02S1 and GYA04	20	18	**9%**	-1300	200
GYA01 failure	20	18	**10%**	600	700
All in well GYA01	20	18	**11%**	700	-700
Double rate	38	26	**31%**	1800	1000
Inject to 2075	62	38	**38%**	1200	300

Table 7-4. Storage capacity results. Summary table for FFM 3.15 (northern pinch-out sensitivity)

FFM 3.15	CO_2 injected (Mt)	Injected CO_2 in original gas zone (Mt)	% CO_2 outside original OWC after injection	Plume extent beyond original OWC –west (m)	Plume extent beyond original OWC –east (m)
Base case	**20**	**18**	**13%**	**1000**	**200**
GYA03 and GYA05	17	15	**13%**	300	-1400
GYA02S1 and GYA04	20	18	**9%**	-1000	300
GYA01 failure	19	17	**11%**	800	300
All in well GYA01	13	13	**2%**	300	-1100
Double rate	30	22	**26%**	1500	800
Inject to 2075	71	39	**46%**	1300	1100

Relevant scenarios are described here in more detail in the following sections.

7.3.1. Base case injection pattern.

When the base case injection pattern (described in (a) above) was run in any of the geological models, the target of 20 million tons of CO_2 was injected, with no egression from the store. For model FFM 3.1, the target was achieved with no backing out of any of the four injection wells and the model indicated a small proportion (13%) of the injected CO_2 lying outside the original OWC at the end of injection. The CO_2 plume reached roughly 700m beyond the original contact in the west, and remained largely within the contact in the east.

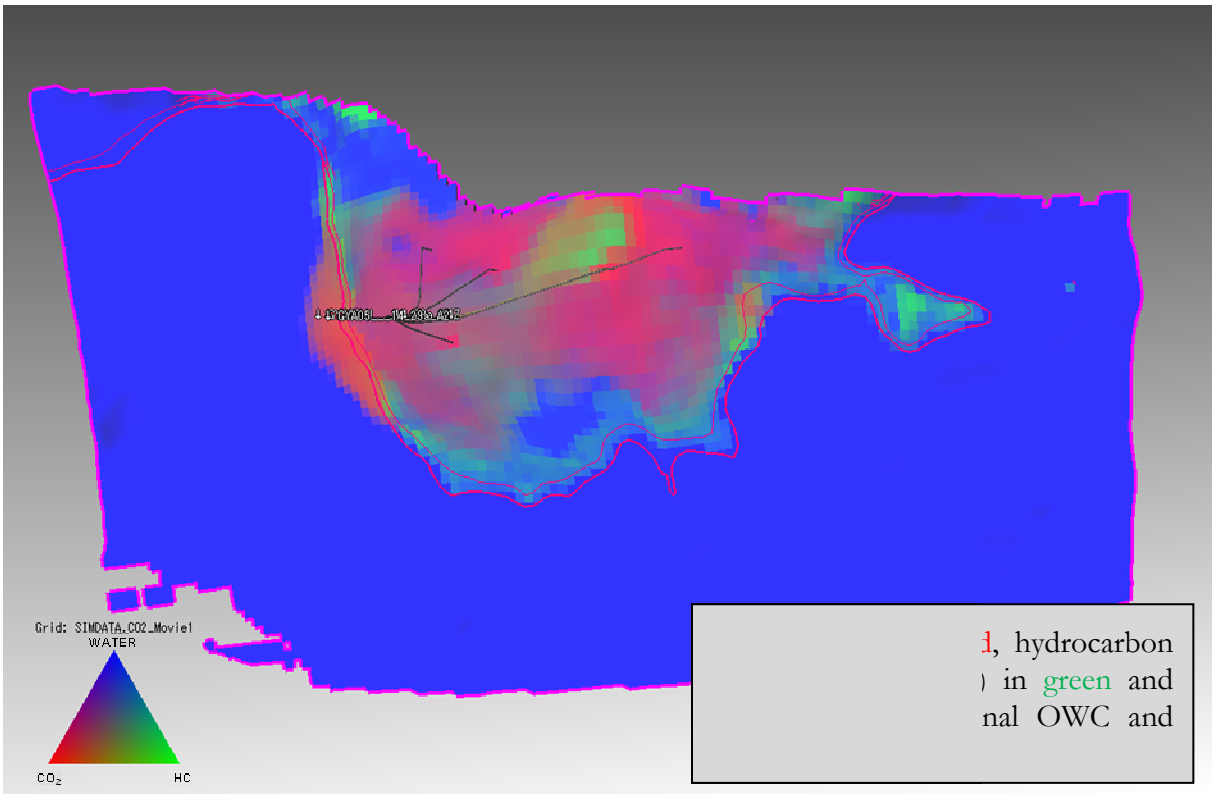

Figure 7-1. FFM3.1: Extent of CO_2 plume at top Captain D, at end of injection (2025).

Note that the colours in all screenshots of fluids in the Goldeneye CCS FFM follow the scheme noted in Figure 7-1 – namely that CO_2 is shown in red, green represents remaining gas or condensate hydrocarbon, water is blue. Original oil/water and gas/oil contacts are shown as pink lines.

Figure 7-1 shows the prediction, from model FFM 3.1, of where CO_2 will be, after injecting a total of 20 Mt in 10 years, using as injectors wells GYA01, GYA02S1, GYA04 and GYA05, with the CO_2 injected equally by each well. This is a simplification of the likely actual injection pattern. For the purposes of this modelling exercise, injection tables representing 4½ inch completions were used. For the simulation, all injectors operated with a BHP constraint of 4000 psi.

Additional simulations were run to assess how the system behaves after cessation of injection. For FFM3.1, all the mobile CO_2 moves back into the hydrocarbon column, with the only CO_2 present beyond the contact being capillary trapped or dissolved in brine. The Figure 7-2 shows how the CO_2 plume recovers back after 10 and 20 years of injection. (The original oil/water and gas/oil contacts are shown as solid lines.)

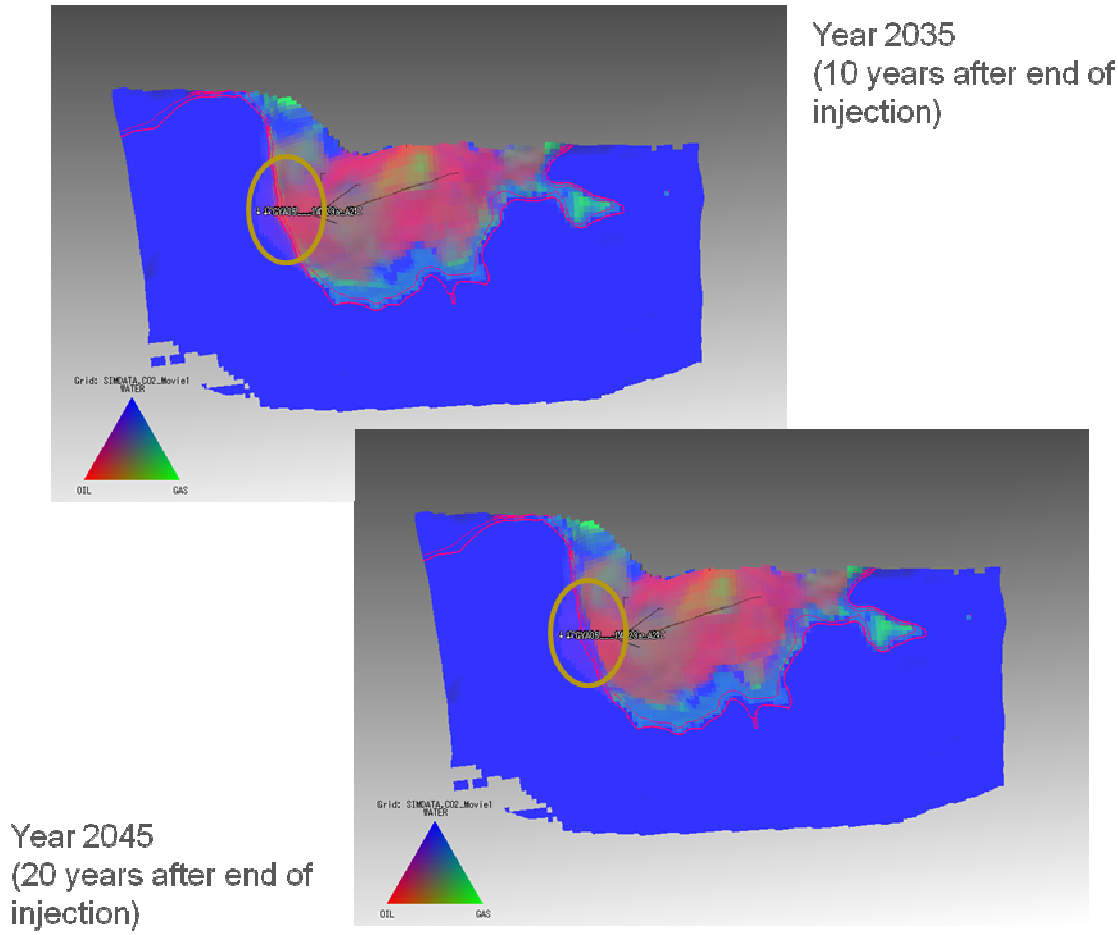

Figure 7-2. FFM 3.1 - CO_2 plume, 10 and 20 years after end injection.

Figure 7-2 shows how even though 13% of the CO_2 injected goes beyond the original oil/water contact into the virgin aquifer beneath the field, extending the plume some 700 m (reference case) outside the initial hydrocarbon area (due to the "Dietz" tonguing effect), it moves back after injection to be constrained within the original hydrocarbon region of the field.

The average reservoir pressure relaxes in the first three to four years after stopping injection (Figure 7-3). In the longer term, the pressure decline slows and becomes a slow recharge, as the larger, and more distant, extended aquifer dominates. This result is supported by work carried out with the extended dynamic model of the larger Captain Fairway aquifer[18].

[18] Dynamic Modelling Report for Goldeneye Project. 2010.

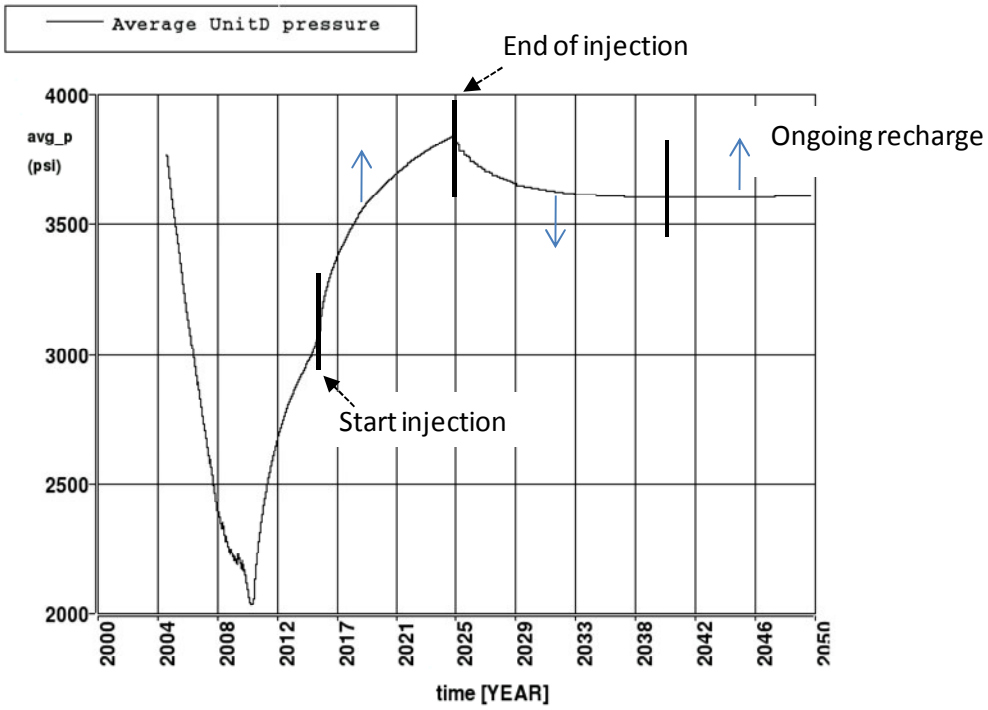

Figure 7-3. FFM 3.1 – recovery of average reservoir pressure (Unit D) after injection.

When the same sensitivity was run in the other two models, the results were very similar. The basic plan of injecting 20 million tons of CO_2, in ten years, using four of the existing wells in Goldeneye, demonstrates no risk of egression when considering alternative geological realisations, meaning that even with a shallower west flank (SRM 3.05) or with a more southerly pinch-out (SRM 3.15) that could make easier for the CO_2 to egress, it still remains within the storage site (see Figure 7-4). As a result, the reference case is a robust CO_2 injection scenario.

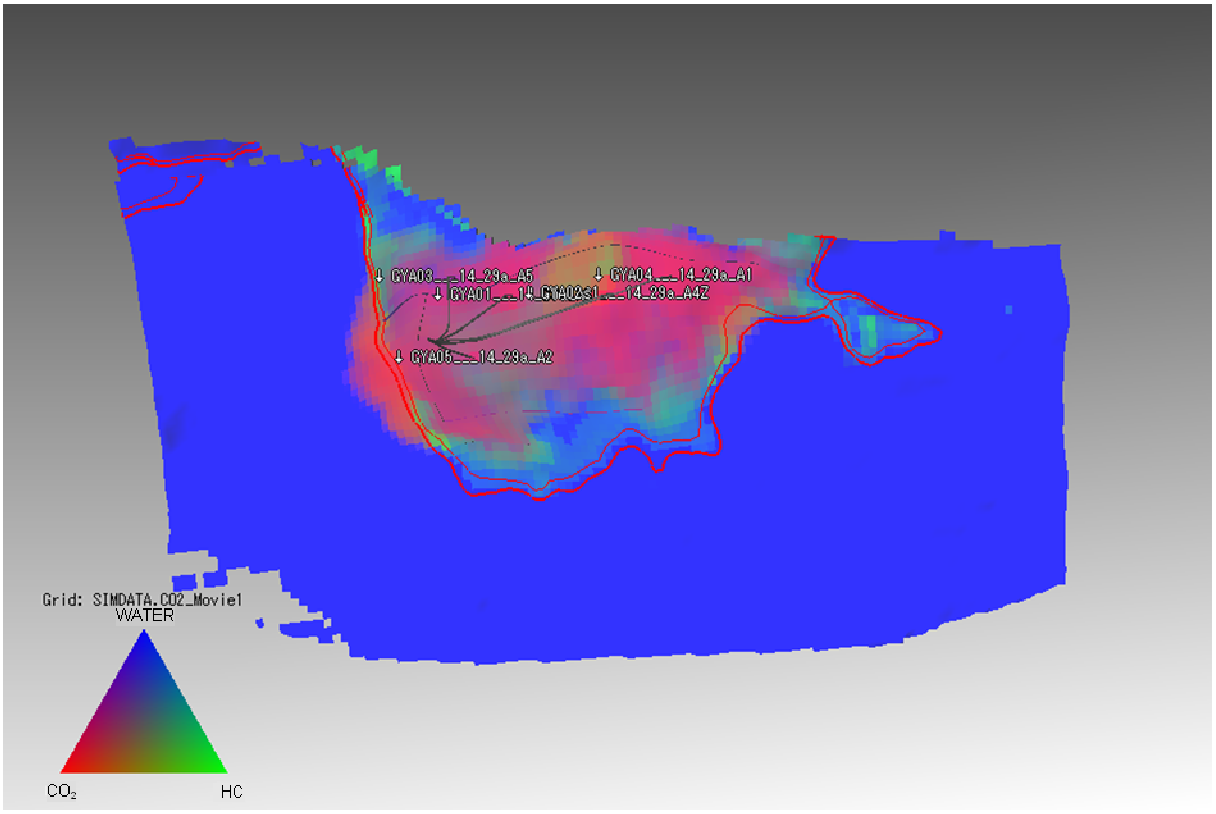

Figure 7-4. FFM 3.15, northern pinch-out sensitivity - Extent of CO_2 plume at top Captain D, at end of injection (2025).

7.3.2. Sensitivity to rate of injection

To investigate the dependency of the system to the (mass) rate of injection of CO_2, the base case injection pattern was run with all injectors operating at double the base rate (i.e. 1,040Mt/year/well). This will not be carried out in reality, as the contract requires 2 Mt/year injection.

Again the extent of the CO_2 plume was checked, plus the average Unit D reservoir pressure, in particular at the point in time when this exceeded the initial pressure (if at all).

For FFM3.1, the average reservoir pressure, after start of injection, reached 3800psi midway through year 2018 with the high rate scenario. With FFM3.15, 3800psi was reached in 2018 (3 months later than FFM31). For FFM 3.05 it was 2023, and the pressure after 10 years of injection was 3884psi.

The lateral extent of the CO_2 plume is also rate dependant. Figure 7-5 illustrates a snapshot of the CO_2 plume at the point in time when 20 million tons had been injected, either at the base case rate or the double rate. This occurs in year 2025 in the base case, and in year 2020 for the high rate case. It can be seen that the Dietz tongue extends a further 200m to the west in the high rate case, illustrating the rate dependence of the CO_2 tongue.

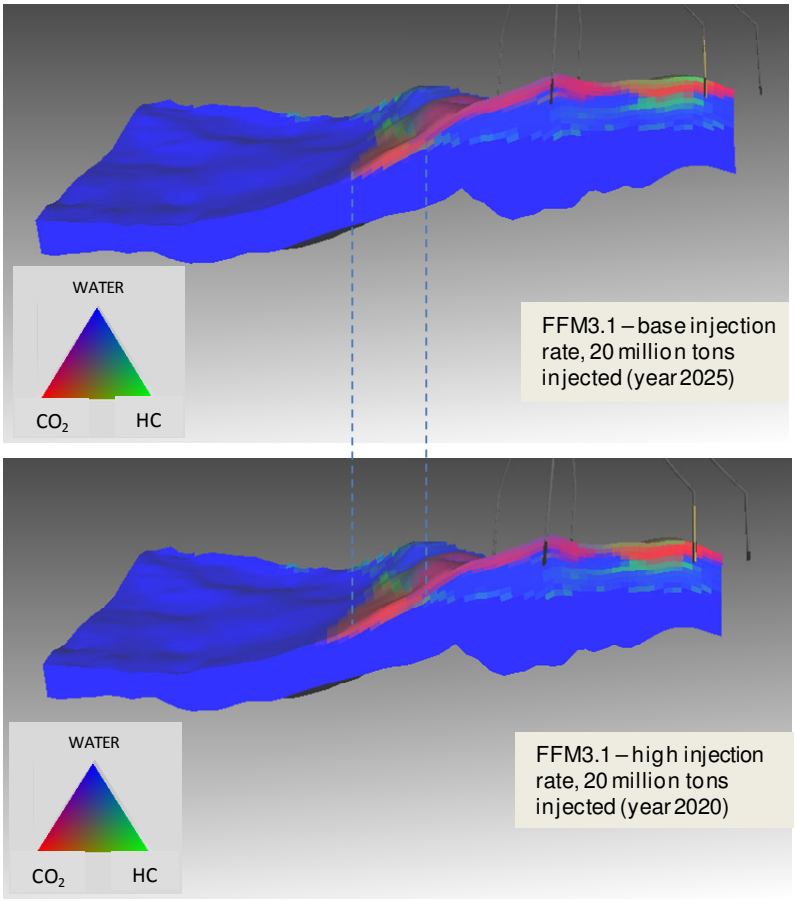

Figure 7-5. FFM 3.1 – Cross section illustrating the Dietz effect.

A higher risk of an egression arises if the total CO_2 is injected at high rate (double the base case rate) for a full 10 years, in the flattest geological realisation (FFM 3.05). However, as shown in Figure 7-6, even in this scenario, the tip of the plume does not reach the spill point and there is no egression.

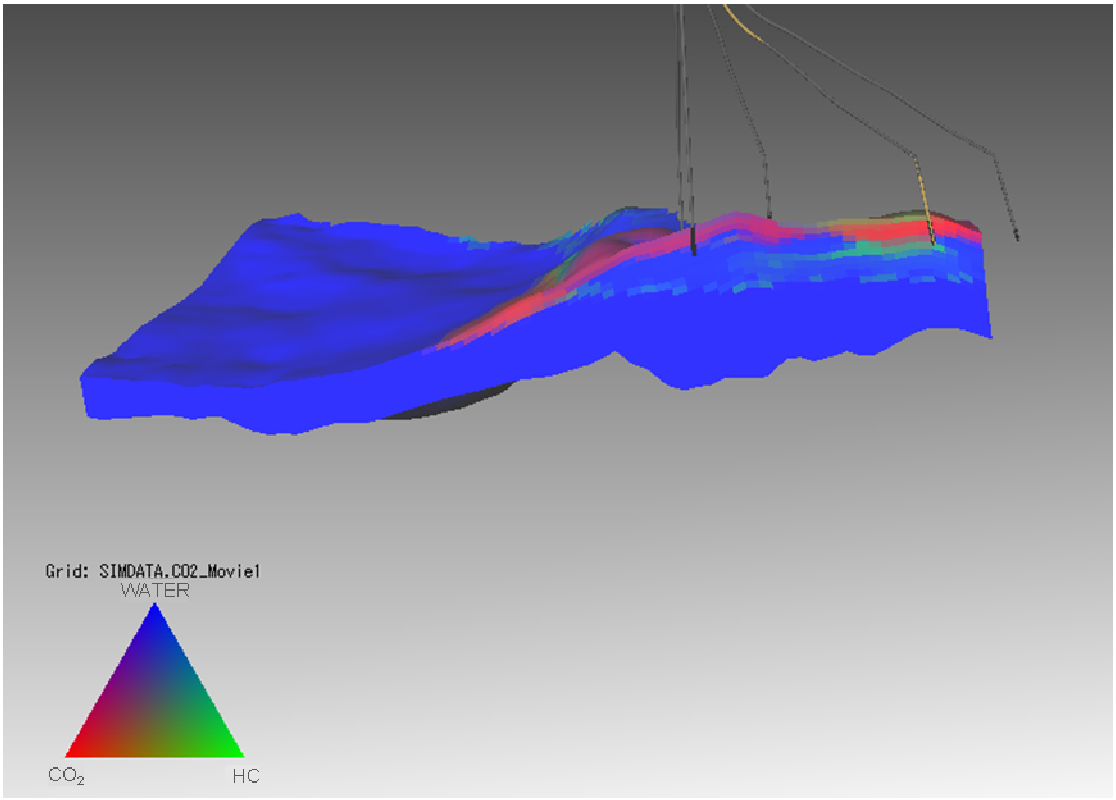

Figure 7-6. FFM 3.05 (west flank sensitivity) – Cross section illustrating the Dietz effect.

In the shallower west flank realisation (FFM3.05) the Dietz tongue is longer after 10 years injection (approx. 1800m from original OWC) than it is in FFM 3.1 (approx. 1400m from original OWC after 10 years injection at high rate).

7.3.3. Maximum storage capacity

To determine a result for the maximum quantity of CO_2 which can be injected without egression from the store, the base case injection scenario was continued past 2025 until the CO_2 plume reached a point from which it could spill out of the store. It was seen that for all geological models, the mass of CO_2, which had to be injected to reach this situation, was significantly higher than the 20 million tons required for this project.

To get an estimate for the maximum storage capacity, which can be made available by appropriate use of the available injection wells, a test injection was done in only wells GYA02S1 and GYA04 – the furthest downdip wells. This is the situation where, the CO_2 plume will be as far away from the structural spill point as possible for each geological model. The maximum storage capacity was estimated by injecting at a total rate of 2 Mt CO_2/year, equally in the two wells (at this rate, the target of 20 Mt CO_2 can be injected in 10 years, as per the competition requirements). Injection is stopped when the tip of the CO_2 plume nears the structural spill point. The wells are then shut in and the system allowed to relax until year 2115. For each geological model, the maximum injected tonnage which does not give rise to egression from the primary store is recorded in Table 7-5.

For the reference case model (FFM 3.1), Figure 7-7 illustrates the extent of the CO_2 plume (at top Unit D) when the maximum storage capacity is reached. With the well pattern and rates described above, this occurs in year 2035 in this case.

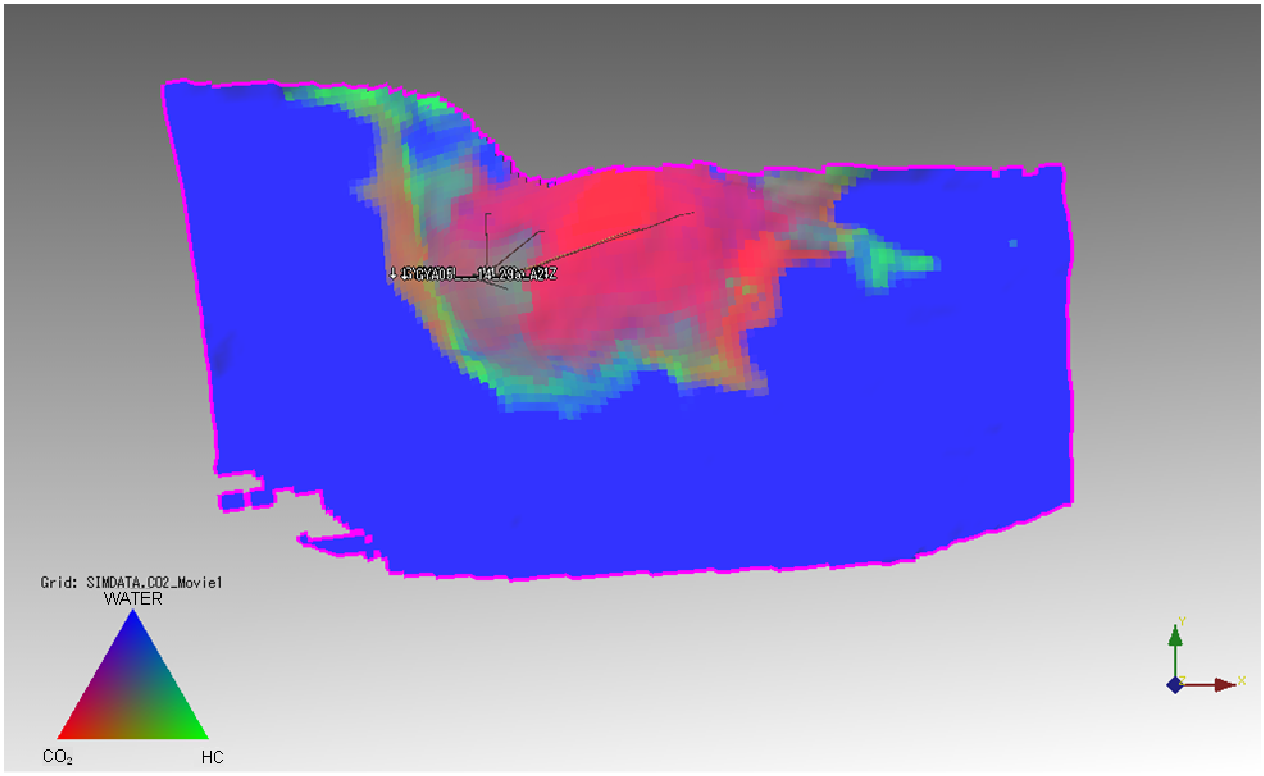

Figure 7-7 **FFM 31 (reference case): CO_2 plume at top D, when maximum storage capacity is reached. Year 2035.**

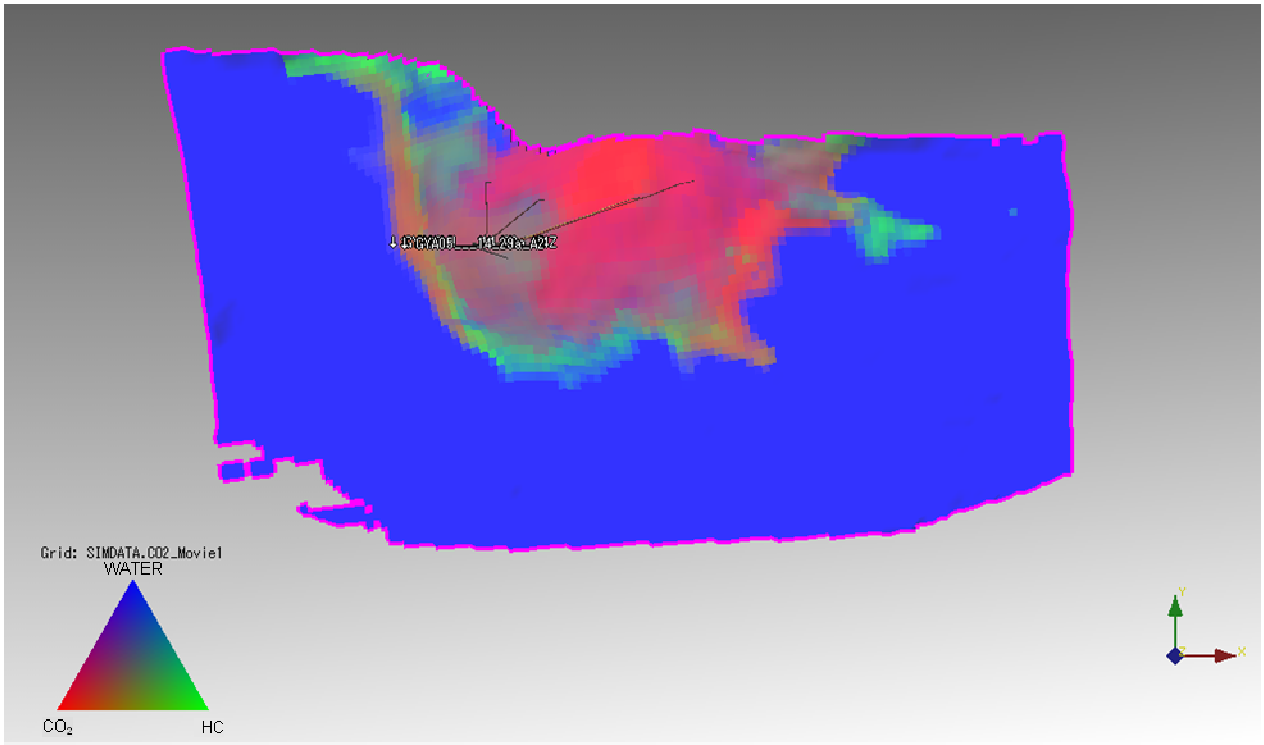

Figure 7-8: **FFM 3.1, CO_2 plume extent five years after ceasing injection when maximum storage capacity was reached. Year 2040.**

Figure 7-8 shows the extent of the plume (at Top D) when the system has relaxed for five years after reaching the estimated maximum storage capacity. The CO_2 is moving back into the original gas cap.

The same effects may be seen in the other geological models. For the case of FFM 3.15, Figure 7-9 shows how the CO_2 redistributes over time between the original water leg and original hydrocarbon gas leg. In this case, 31 Mt are still resident in the original gas zone after 100 years, and 7 Mt in the original water zone. This graph includes the CO_2 present in the system before commencement of injection – a total of roughly 0.1 Mt, of which 7% was in the original water zone.

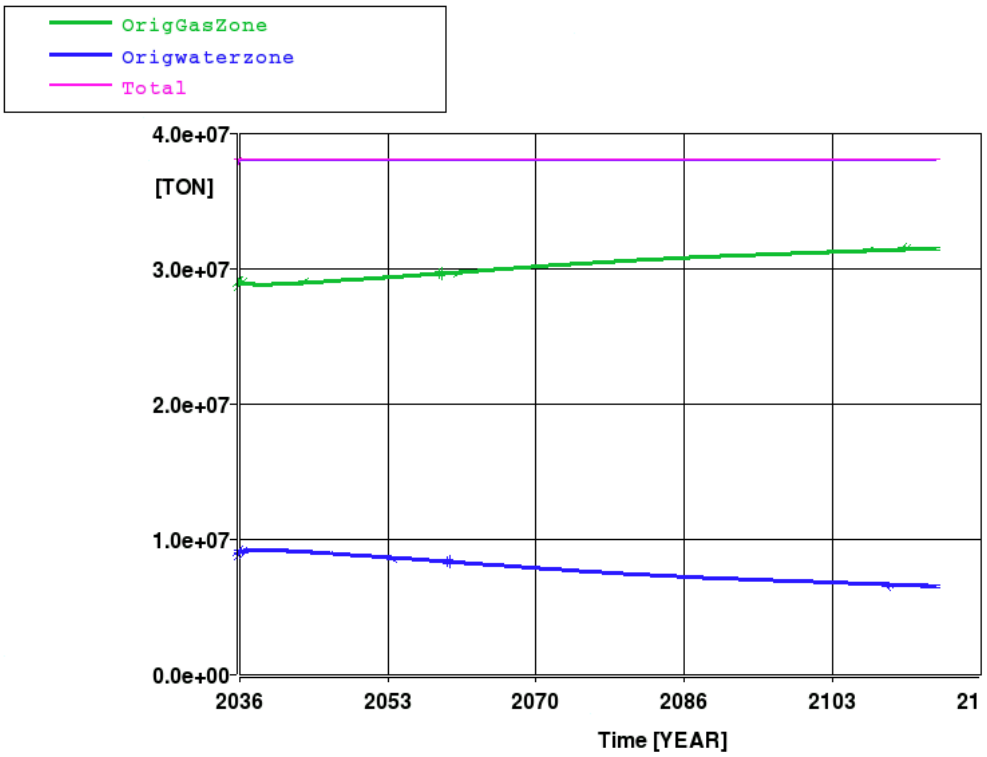

Figure 7-9: (FFM 3.15) - redistribution of CO_2 with time after cessation of injection.

This maximum storage capacity test was carried out for all three geological models. The results are summarised in Table 7-5. In each case, the total CO_2 stored is listed, together with the mass of injected CO_2 which is resident in the original water zone at 1.1.2115 (i.e. excluding the CO_2 present in the reservoir before injection). The lowest estimated storage capacity here occurs for FFM 3.05. This model was constructed with a shallower slope on the western flank, and it was expected that it would be easier for CO_2 to leave the geological storage (section 5.2).

Thus there is a substantial storage margin – it is possible to inject between 11 Mt and 18 Mt CO_2 over that required for this project.

Table 7-5. Estimate of maximum storage capacity.

Geological model	Maximum CO_2 injected to reach spill (Mt) - in original gas and water zones.	Injected CO_2 resident in original water zone after relaxing to 1.1.2115 (Mt)
FFM 3.1	36	6
FFM 3.05	31	3
FFM 3.15	38	7

7.3.4. Failure of one injector

To test this sensitivity, each one of the four injectors is switched off after 5 years of injection, and replaced by well GYA03 (which does not inject in the base case) injecting at the same rate. A key point to look out for is the final distribution of the CO_2 plume.

One instance is the failure of well GYA01. In FFM 3.1, it was still possible to inject a total of 20 million tons of CO_2. Even in the extreme cases of a shallower flank (FFM 3.05) or a more southerly pinch-out (FFM 3.15), it was possible to inject the tonnage committed.

Table 7-6. Failure of well GYA01

Geological model	CO_2 injected with failure of GYA01 (Mt)	CO_2 outside original OWC at end of injection (Mt) (% total injected)
FFM 3.1	20	3 (12%)
FFM 3.05	20	2 (10%)
FFM 3.15	20	2 (12%)
FFM 3.1 – reference case, no well failure	20	3 (13%)

7.3.5. Well injection pattern

This is a test of the sensitivity of the system to the exact selection of the wells used for injection. In one case, all the CO_2 is injected equally into wells GYA03 and GYA05, to the west of the field. In another, the same condition was run with wells GYA04 and GYA02S1 – to the east. A series of further sensitivities pushed this idea to the extreme by injecting all the CO_2 in one well only (each of the five wells was tested in this way).

7.3.5.1. Injecting into GYA03 and GYA05

In none of the runs with this injection pattern did the CO_2 plume reach the spill point. However, the total quantity injected was lower than the target 20Mt in one case – FFM 3.15.

Table 7-7. Injection in wells GY03 and GYA05 only

Geological model	CO_2 injected using GYA03 and GYA05 only (Mt)	CO_2 outside original OWC at end of injection (Mt) (% total injected)
FFM 3.1	20	4 (21%)
FFM 3.05	20	3 (18%)
FFM 3.15	17	2 (13%)
FFM 3.1 – reference case, 4 injectors	20	2 (13%)

The extent of the plume in FFM 3.15 is considerably less than the other two, largely due to the fact that less CO_2 was injected, and this is turn is due to the performance of well GYA03. In FFM 3.1, well GYA03 injected 10 Mt, but only 6.6 Mt in FFM 3.15. Well GYA05 injected the same tonnage in each case. The permeability in the region of well 3 is on average lower in FFM 3.15 than in FFM 3.1 (Figure 7-13), hence lower injectivity for this well in FFM 3.15.

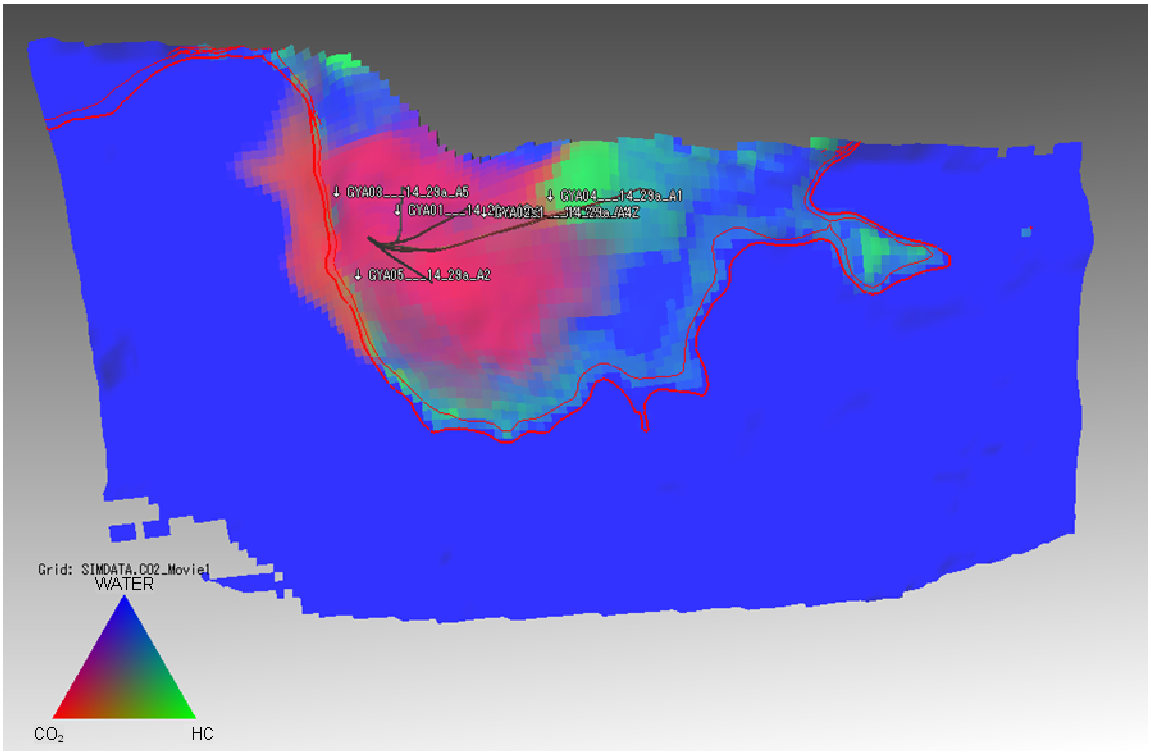

Figure 7-10. FFM3.1, injecting in GYA03 and GYA05 only.

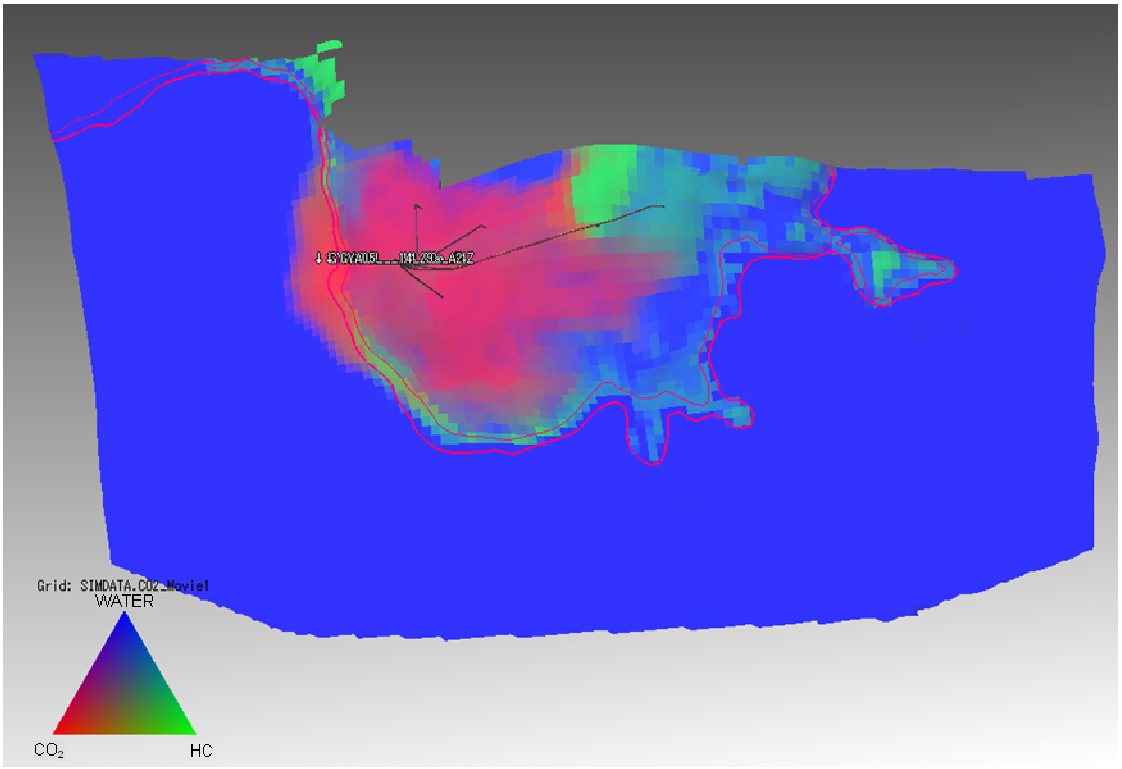

Figure 7-11. FFM 305, injecting in GY03 only and GYA05 only.

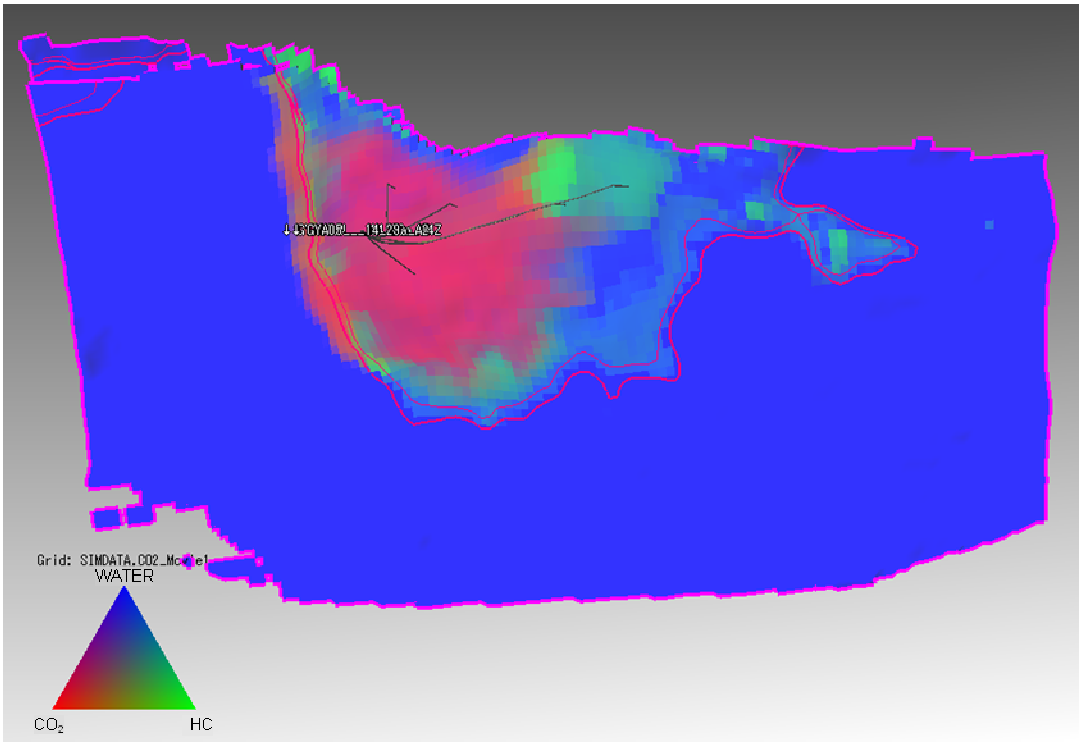

Figure 7-12. FFM 3.15 (northern pinch-out sensitivity), injecting in GYA03 and GYA05 only.

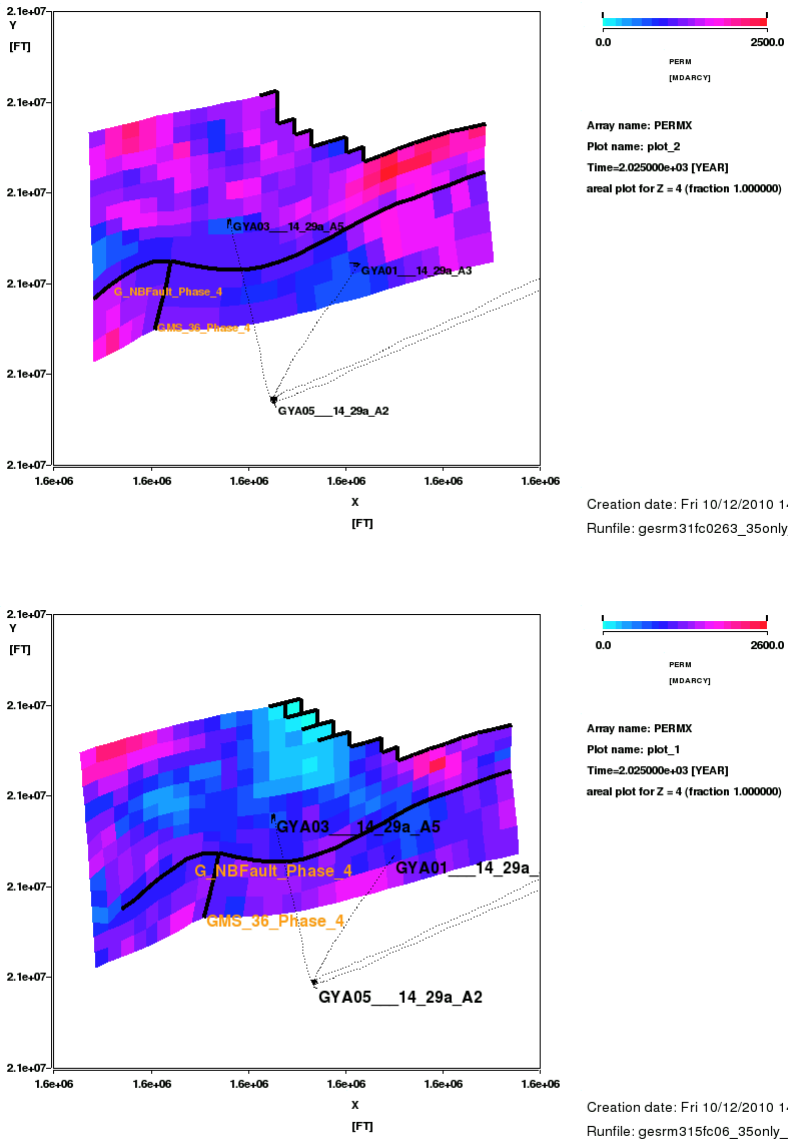

Figure 7-13. Plane view in region of well GYA03 in FFM 3.1 (top) and FFM 3.15 (bottom), illustrating the differences in permeability around the well in each model.

Nevertheless, it is understood that this lower permeability in SRM 3.15 is a feature generated within the simulation model. The pinch out sensitivity was created by setting NTG property to zero north of the new pinch-out line, so it is a "property pinch out" instead of a "stratigraphic pinch out" as it is officially interpreted. This was a model simplification because creating different pinch out by modifying the structure was too complicated. As a consequence, the re-population of petrophysical properties in the realization was somehow slightly altered due to this change. With strictly correct modelling GYA03 should not have injectivity restrictions, hence the tonguing effect (Dietz tongue) should be very similar to that observed in the reference case (SRM 3.1).

7.3.5.2. Injecting into GYA02S1 and GYA04

All cases studied were able to achieve the target of 20 million tons CO_2 with good containment. There were few differences in the key results for each case.

Table 7-8. Injection in wells GY02S1 and GYA04 only

Geological model	CO_2 injected using GYA02S1 and GYA04 only (Mt)	CO_2 outside original OWC at end of injection (Mt) (% total injected)
FFM 3.1	20	2 (9%)
FFM 3.05	20	2 (9%)
FFM 3.15	20	2 (9%)
FFM 3.1 – reference case, 4 injectors	20	3 (13%)

The more favourable results for containment (compared with the reference case or injection in wells GYA03 and GYA05) are largely due to the location of these two wells, more being central and higher in the structure. They are less dependent on the nature of the western flank or northern pinch-out (both key geological uncertainties). However, using wells GYA02S1 and GYA04 does cause greater degree of egression over the eastern flank. If the total injection is spread more evenly over the structure, there is less impact on the east. The example of FFM 3.1 is shown in Figure 7-14.

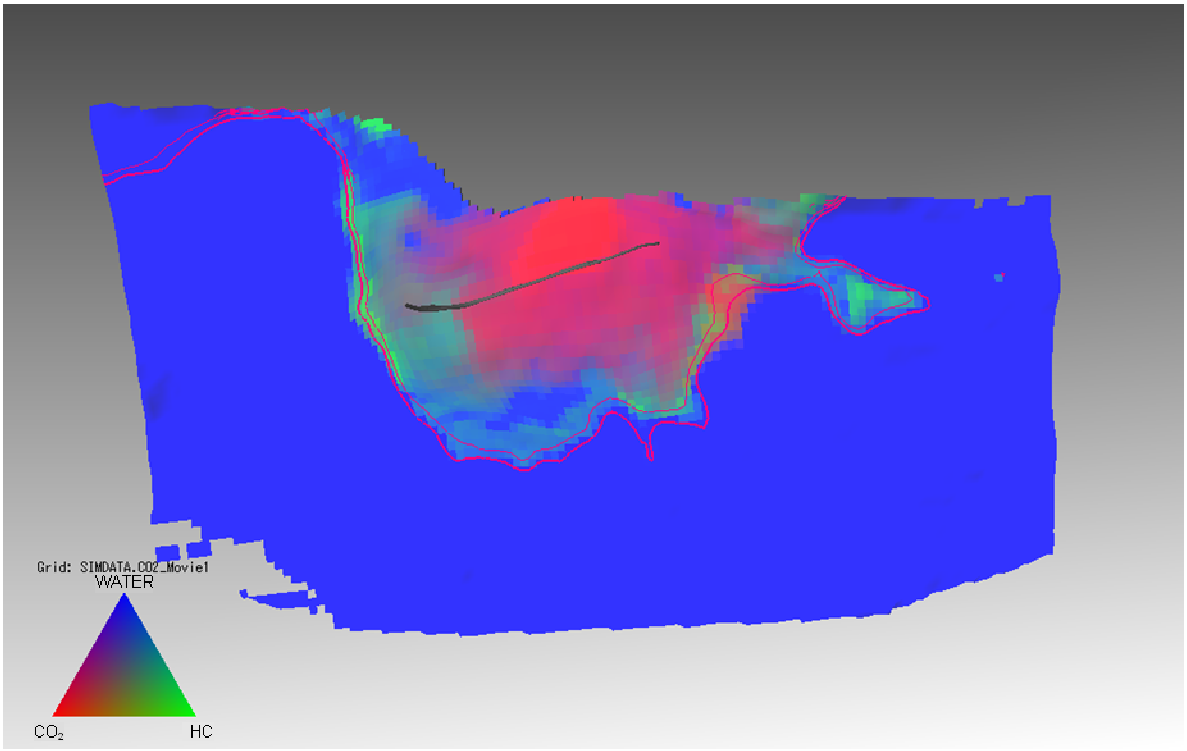

Figure 7-14. FFM 3.1 (reference case)- injecting equally in wells GYA02S1 and GYA04 only.

7.3.5.3. Injecting into one well only

As an extreme case, simulations were run attempting to inject 20 million tons CO_2 into one well only. In general, it was not possible to meet the target completely with only one well. However, this situation is unlikely to be attempted in reality.

For example – injecting in well GYA01 only – a crestal well. The results for mass stored are shown in Table 7-9.

Table 7-9. Injection with one well only (GYA01)

Case	Mass CO_2 stored (million tons)
FFM31	14
FFM315	14
FFM305	20

Even though the sequestration target of 20Mt was not achieved, the test of injecting the highest volume into a single well still does not results in egression from the container. (Figure 7-15)

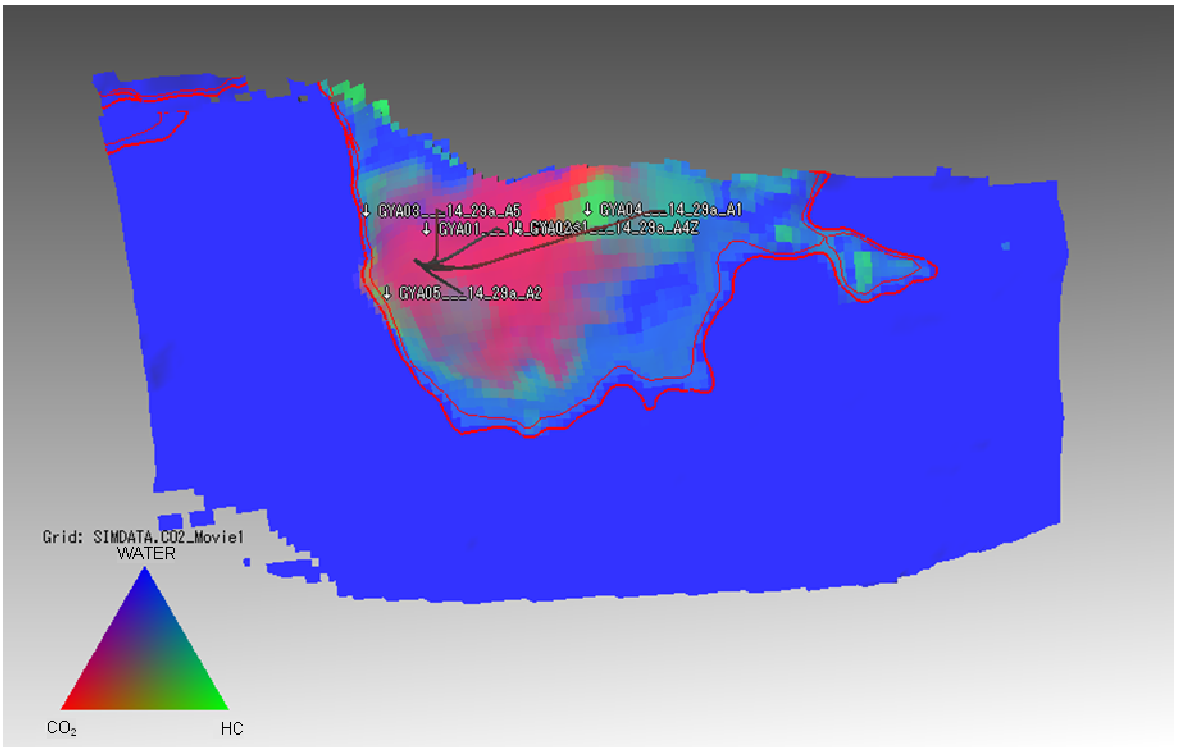

Figure 7-15. FFM 3.15 (northern pinch-out sensitivity) – injection in well GYA01 only. CO_2 plume after 10 years injection (top Unit D).

7.4. Well completions

Once information on the proposed well re-completions became available, it became possible to repeat this modelling exercise using alternative well parameters. This exercise was important in order to check that the encouraging findings on robustness were still valid.

The injection tables which had been used for the study up to this point (designed for generic 4½ inch completions) were replaced by those appropriate for the planned completions. Maximum gas injection rates were set for each of the wells (Table 7-10).

Table 7-10. Maximum injection rates for well completions scenario

Well	Max. rate [Mscf/day]	Max. rate [Mt/year]
GYA01	50,000	1.0
GYA02S1	35,000	0.7
GYA04	40,000	0.8
GYA05	27,000	0.5

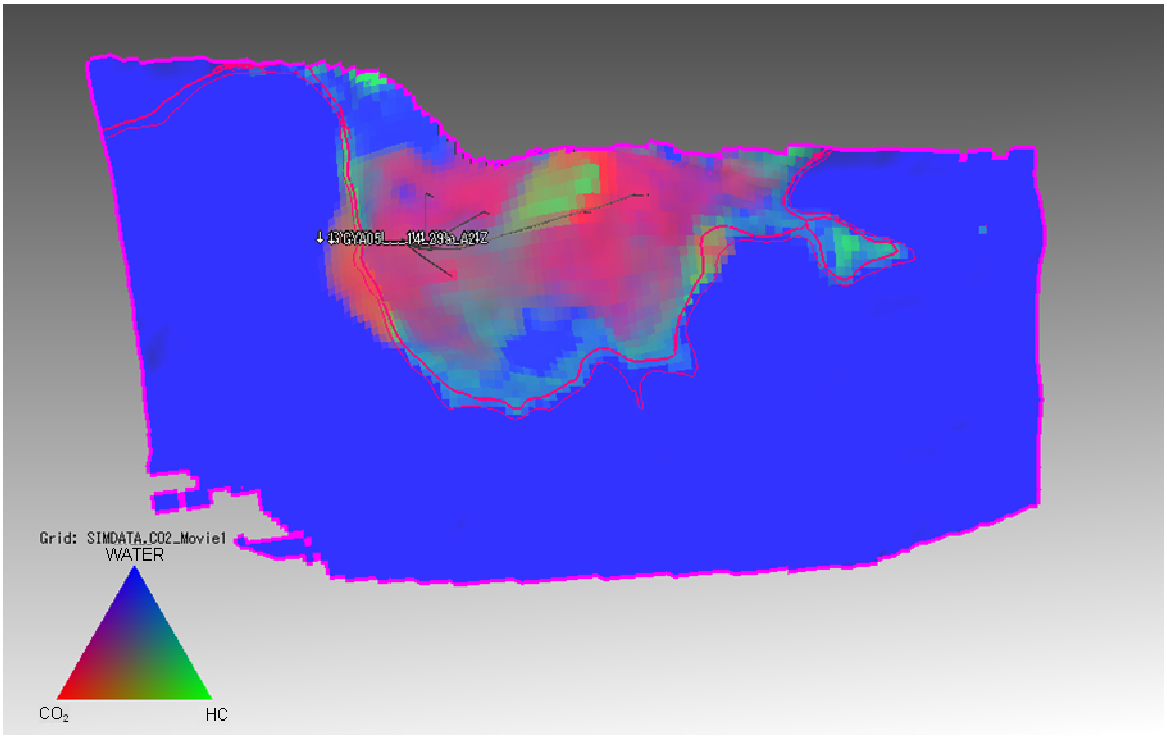

Figure 7-16. FFM 3.1, realistic scenario, CO_2 plume after injection. Original OWC and GOC in red.

After injection of 20 Million Tonnes CO_2 in this scenario, 15% of the CO_2 (3 Million Tonnes) was outside the original gas zone.

This was a first attempt at modelling the actual well performance, using mass rate constraints on each well and updated injection tables. The same well sequence as that adopted in all the sensitivities shown here was used, with no attempt yet made to refine it. During detailed design further work will

be required in order to optimise the well sequence, but at this point the scenario does not display shortcomings.

7.5. CO_2 Dissolution

Most of the sensitivities do not include CO_2 dissolution in water. This effect will increase the storage capacity of the reservoir and trap more of the CO_2 over time after injection ceases. As well as trapping CO_2 in solution, dissolution also results in an increase in the water density which can introduce buoyancy driven convection currents, although this is only significant over time periods longer than the 10 year injection period. MoReS includes a CO_2 dissolution option and this has been used to investigate the effect of dissolution by re-running the injection Base Case with CO_2 dissolution switched on.

Figure 7-17 illustrates the CO_2 distribution at the end of injection in 2025 with CO_2 dissolution active. CO_2 is shown in red. Green represents remaining gas or condensate hydrocarbon. Comparison with Figure 7-1 shows that there is very little difference in the extent of the CO_2 plume.

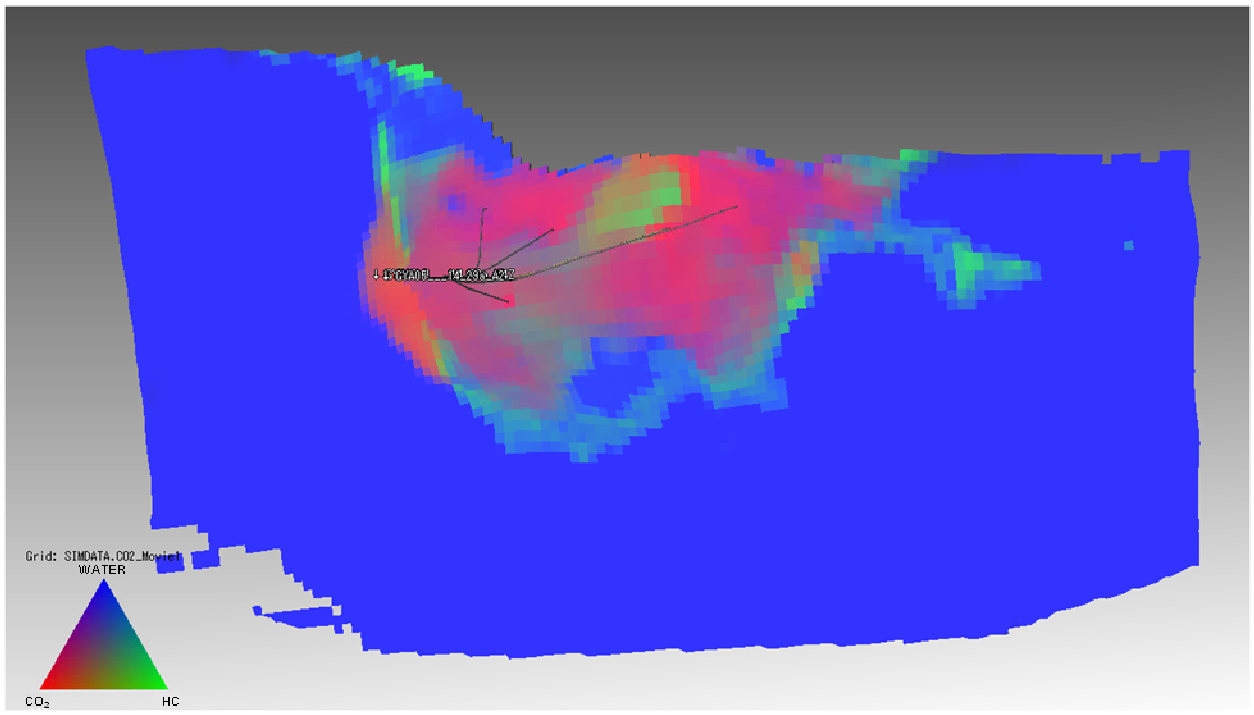

Figure 7-17. FFM 3.1: Extent of CO_2 plume at top Captain D at end of injection with dissolution.

Figure 7-18 illustrates the mass of CO_2 dissolved in water in both the gas zone and the water zone outside the gas plume. In 2025 after 10 years injection, 0.1 Million Tonnes CO_2 has dissolved in water outside the gas plume while 0.9 Million Tonnes of CO_2 has dissolved in water in the gas plume. A total of ~1 Million Tonnes of CO_2 is dissolved in water (approximately 5% of the injected volume).

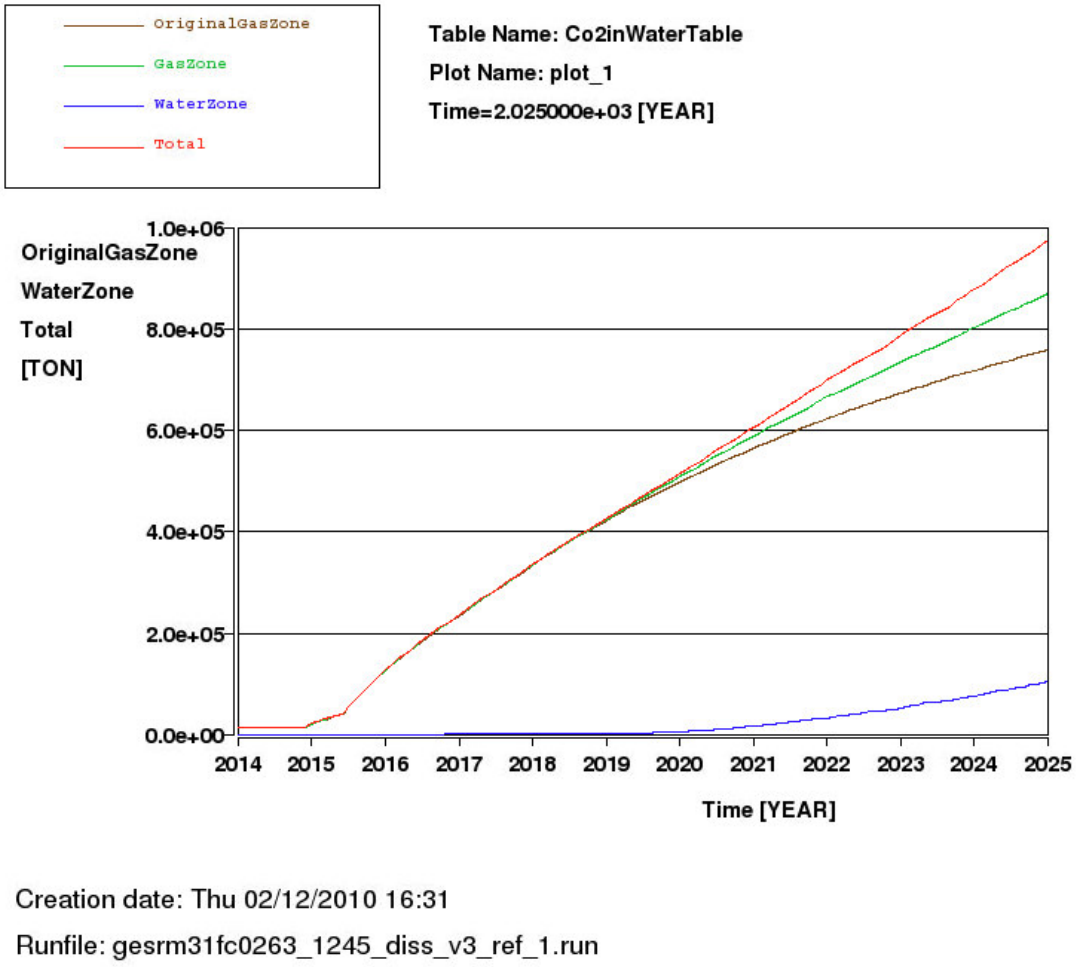

Figure 7-18. FFM 3.1 (Reference case) Mass of CO_2 dissolved in water during 10 year injection period.

In Figure 7-18 the Gas Zone is the part of the reservoir where the original S_g>0.01[19] and the Water Zone is where S_w>0.99[20].

Figure 7-19 shows the change in the mass of CO_2 dissolved in water when the reservoir is left to equilibrate for 1000 years after injection. The total volume dissolved in water gradually increases to 1.9 Mt over the period, nearly double the initial amount of CO_2 dissolved in water. Nearly all of the extra dissolution takes place in the Water Zone as the water in the gas plume is already saturated.

The volume of CO_2 dissolved in water is overestimated in the simulation mainly due to the fact that all the CO_2 in a block is assumed to be in contact with the water and the CO_2 saturation of the water immediately increases to the maximum amount allowed by the mass of CO_2. In reality, the CO_2 will not be in immediate contact with the water. The solubility is higher than that calculated using the correlation of Chang, Coats and Nolen[21] [Spreadsheet calculations using this correlation suggest that only 2.2% of the CO_2 will initially dissolve in water].

[19] Gas saturation

[20] Water saturation

[21] Chang, Y-B, Coats, B. K. and Nolen, J. S.: A Compositional Model for CO_2 Floods Including CO_2 Solubility in Water. SPE Reservoir Evaluation and Engineering. April 1998.]

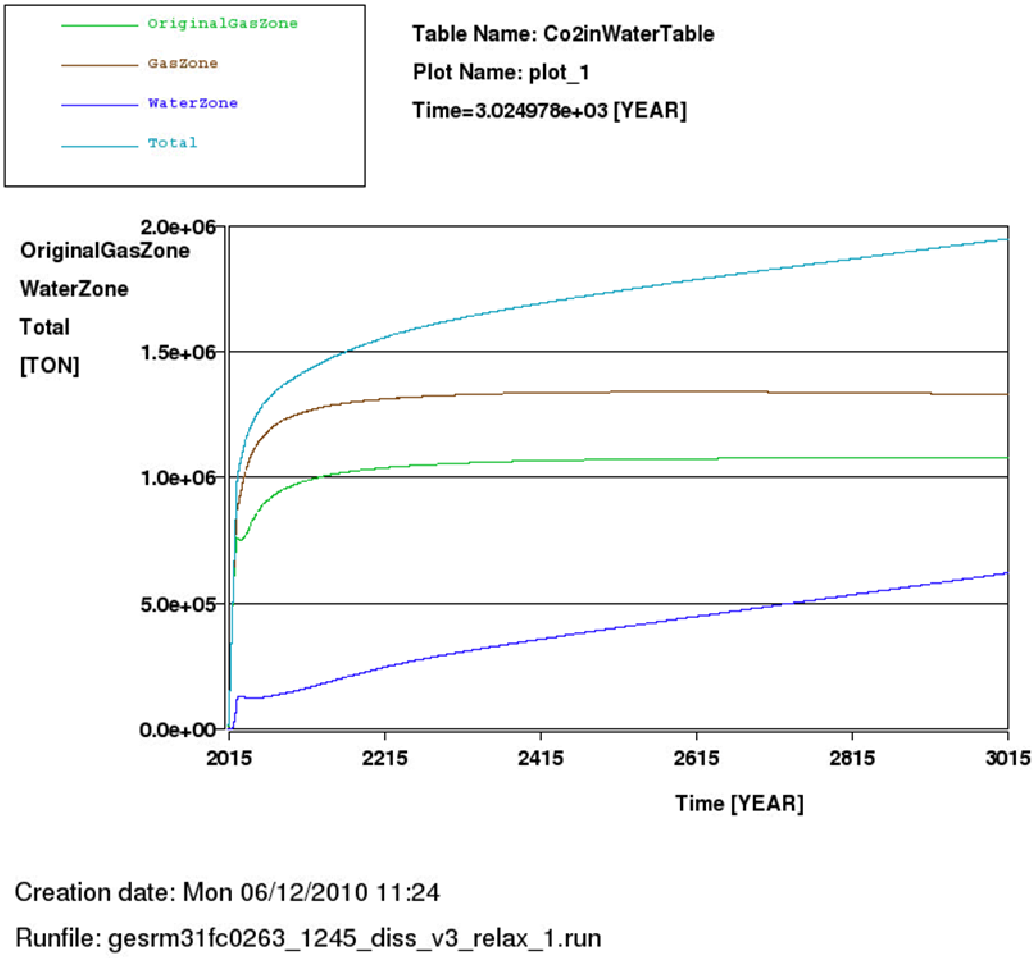

Figure 7-19. FFM 3.1 (Reference case): Mass of CO_2 dissolved in water during 1000 years.

In Figure 7-19, the Gas Zone is the part of the reservoir where the original S_g>0.01 and the Water Zone is where S_w>0.99.

8. CONCLUSIONS

Geologic carbon storage capacity has been calculated for the Goldeneye reservoir, resulting in **47 million tonnes of CO_2** equivalent available for storage as maximum theoretical boundary.

This maximum storage volume initially estimated was modified by storage efficiency factors which account for the fact that CO_2 may not be able to completely refill this volume.

The major static elements that could impact the storage capacity of Goldeneye are: (a) extension of the stratigraphic pinch-out; (b) structural dip on the western flank of the field; and (c) internal Captain Sand stratigraphy (thickness). Dynamic elements have also been considered and are mainly related to the displacement mechanism and the unfavourable mobility ratio of the process. These elements are summarised in: (a) relative permeability end points (both water and gas/CO_2), and (b) residual gas saturation (S_{gr}).

The conjunction of these static and dynamic uncertainties depicts the framework which is necessary for understanding the storage efficiency factors that discount the total theoretical capacity.

A three-dimensional, three-phase, full field Goldeneye numerical simulation model corroborated the initial storage estimations and evaluated different injection scenarios to map out the range of capacity available for CO_2 storage.

The complete suites of static reservoir models created to investigate CO_2 injection performance in the field demonstrate that Goldeneye has sufficient storage capacity to **hold 20 million tonnes of CO_2,** as mandated by the UK CCS Demonstration Project. All of the uncertainty scenarios currently evaluated showed that the field can safely sequester the intended volume.

In addition to the storage capacity defined by the structural trap of Goldeneye, the water leg beneath the reservoir (that lies within the storage site) could also account for extra capacity, based on numerical simulation results.

Just a small proportion (13%) of the total injected CO_2 lays outside the original OWC at the end of injection. However, after the cessation of injection all the CO_2 is either recovered back into the geological store or is otherwise sequestered (by means of dissolution or capillary trapping).

In order to determine the maximum geologic carbon storage capacity for the Goldeneye reservoir, a theoretical continuous CO_2 injection until 2035 scenario (20 years of injection) revealed that over **30 million tons of CO_2** had to be injected to reach the structural spill point and create an egression. This considers a combined Goldeneye hydrocarbon reservoir in addition to the storage capacity of the aquifer beneath the field. The figure represents at least **50% storage capacity margin** to the storage complex, giving confidence that Goldeneye can safely sequester the 20 million tonnes of CO_2 as mandated by the UK CCS Demonstration Project.

9. Glossary of terms

CCS	Carbon Capture & Storage
FEED	Front End Engineering Design
IIP	Initially In-Place (volumes)
CO_2	Carbon Dioxide
SRM	Static Reservoir Model
FFM	Full Field Model
EOFL	End Of Field Life
CoP	Cessation of Production
GIIP	Gas Initially In-Place
PVT	Pressure, Volume, Temperature
Mscf	Thousand cubic feet at standard conditions
Mcf	Thousand cubic feet at reservoir conditions
EUR	Estimated Ultimate Recovery
Sm^3	Cubic metre at standard conditions
Mt	Million Metric Tonnes
OWC	Oil Water Contact
OOWC	Original Oil Water Contact
TVDSS	True vertical depth sub sea
MoReS	Modular Reservoir Simulator

In the text well names have been abbreviated to their operational form. The full well names are given in **Table 7-1**.

Volumes quoted at 'standard conditions' assume temperature of 60°F and pressure of 14.7psia.

Full name	Abbreviated name
DTI 14/29a-A3	GYA01
DTI 14/29a-A4Z	GYA02S1
DTI 14/29a-A4	GYA02
DTI 14/29a-A5	GYA03
DTI 14/29a-A1	GYA04
DTI 14/29a-A2	GYA05

Table 9-1 Well name abbreviations